6-2017

Effects of eggshell removal on embryonic skeletal development in the American alligator (Alligator mississippiensis)

Nelson Armando Membreno
California State University - San Bernardino, membrenn@coyote.csusb.edu

EFFECTS OF EGGSHELL REMOVAL ON EMBRYONIC SKELETAL DEVELOPMENT IN THE AMERICAN ALLIGATOR (*ALLIGATOR MISSISSIPPIENSIS*)

A Thesis

Presented to the

Faculty of

California State University,

San Bernardino

In Partial Fulfillment

of the Requirements for the Degree

Master of Science

in

Biology

---

by

Nelson Armando Membreno

June 2017

EFFECTS OF EGGSHELL REMOVAL ON EMBRYONIC SKELETAL DEVELOPMENT IN THE AMERICAN ALLIGATOR (*ALLIGATOR MISSISSIPPIENSIS*)

A Thesis

Presented to the

Faculty of

California State University,

San Bernardino

---

by

Nelson Armando Membreno

June 2017

Approved by:

Dr. Tomasz Owerkowicz, Committee Chair, Biology

Dr. Stuart Sumida, Committee Member

Dr. Angela Horner, Committee Member

Dr. Kristopher Lappin, Committee Member

ABSTRACT

The eggshell of reptiles is essential for not only protecting the embryo, but can also serve as source of calcium for embryonic skeletal development. Whereas embryonic lepidosaurs and chelonians rely on their yolk sac for calcium during development, embryonic archosaurs mobilise eggshell calcium supply to both the embryo and the yolk sac. By the time archosaurs hatch, their residual yolk sacs have a calcium content equal or greater than at time of oviposition, which is used to support post-hatching growth. To date, no study has looked into how removal of the calcareous eggshell affects embryonic development in archosaurs. I tested how the removal of the calcareous eggshell affects embryonic and hatchling growth and biomechanic function of the skeleton in embryos and hatchlings of the American alligator (*Alligator mississippiensis*). Experimental eggs had their eggshell manually peeled, while control eggs were sham handled but otherwise not altered. Sampling of eggs occurred on a weekly basis until the end of incubation. Embryos, yolk sacs, and eggshells were removed and analyzed for morphological, histological and biomechanical parameters. Results show that at the time of eggshell peeling yolk sac calcium reserves were sufficient for experimental embryos to develop, but animals hatched in diminutive state. Serial clearing and staining of embryos revealed that onset of bone mineralization was similar for both treatment groups. Growth trajectory of experimental hatchlings parallelled that of control animals, without compensatory growth. Experimental hatchlings were observed to have flexible

lower jaws and produced a weaker bite force than control hatchlings. Cross-sections of the mandible and femoral mid-diaphysis had a significantly reduced cross-sectional area in experimental hatchlings. I conclude that loss of the calcareous eggshell during incubation leads to severe constraint on growth and biomechanics of the alligator skeleton.

ACKNOWLEDGEMENTS

I would like to express my sincerest gratitude to my thesis advisor Dr. Tomasz Owerkowicz. It is from taking his graduate course in vertebrate physiology during my first year that I realized that it was the field of biology I wanted to focus on. Before taking his class I wanted to become a geneticist and now I am excited to continue to explore the world of whole organismal biology. I am also very grateful for our numerous discussions on science, work, and life in general. Under his tutelage I have gained a better understanding of how science works and feel that I have grown as a biologist.

I would also like to thank my committee members, Dr. Stuart Sumida, Dr. Angela Horner, and Dr. Kris Lappin — Dr Sumida for letting me TA lower division human anatomy and physiology lab and learn how exciting teaching anatomy can be, Dr. Horner for her helpful insights into biomechanics, and Dr. Lappin for providing the bite-force transducer I needed to measure my hatchlings' max bite-force. I would also like to thank Dr. Ruth M. Elsey for providing the alligator eggs.

I of course would like to thank my fellow lab mates, Johnny Yang, Jessica Joneson, Krista Felbinger, Elisabeth Cook, and Dorothy Skates as well as the numerous undergrads that assisted me in acquiring and prepping my specimens for this project. Lastly, I would like to give a special thanks my family members and best friends Roger Portillo, Albert Sierra, and Terry McBride for being supportive and pushing me forward.

TABLE OF CONTENTS

LIST OF TABLES

LIST OF FIGURES

CHAPTER ONE

INTRODUCTION

The Cleidoic Egg

The vertebrate egg can be defined as cleidoic or non-cleidoic depending on the materials it exchanges with its environment. Needham (1931) defined the cleidoic egg as a closed box in which all of the nutrients needed for embryonic development are contained within and the embryo primarily exchanges respiratory gasses with the surrounding environment. In contrast, a non-cleidoic egg exchanges gases, water, and other molecules with its environment. The eggs of most oviparous amniotes are cleidoic and are generally composed of an outer eggshell (calcified to variable extent, depending on the species), inner fibrous shell membrane, and egg contents: embryo, albumen, and yolk (Stewart, 1997). Monotremes are the only known extant mammals to lay eggs. The eggshell of the platypus, *Ornithorhynchus anatinus*, lacks a calcareous layer but has a thin shell membrane consisting of an inner basal layer, a middle rodlet layer, and an outer matrix layer (Hughes, 1984).

The eggs of oviparous amniotes are different from those of fish and amphibian eggs, which consist of an outer jelly capsule, an inner vitelline membrane, perivitelline space and yolk (Packard and Seymour, 1997). The morphology of the amphibian egg requires that it be laid in or near water for the embryos to develop. Without a source of water, amphibian eggs will desiccate. The total size of the egg is limited due to the jelly capsule which needs to be thick

enough to support the egg but not so thick as to hinder diffusion of respiratory gases (Seymour and Bradford, 1995). The appearance of the eggshell allowed for limited water loss and helped free amniotes from being confined to reproduce near sources of water. The amniote extraembryonic membranes also compartmentalized various aspects of the egg contents. The embryo resides in the fluid filled amnion, most of the nutrients for development are stored in the yolk sac, waste products are stored in the allantois, and the chorioallantoic membrane (fusion of the chorion and allantois) facilitates gas exchange between the egg and the environment (Stewart, 1997). The eggshell itself not only protects the embryo from desiccation and mechanical damage but can also prevent pathogens from infecting the egg as seen in the eggs of mound building birds (D'Alba et al., 2014). Finally, the eggshell (along with the yolk sac) serves as a source of calcium for the developing embryo.

The calcareous eggshell layer of oviparous reptiles varies in the degree of mineral content, the arrangement of mineral crystals, and nature of mineral itself. The eggshell is composed of an outer inorganic layer and an inner organic fibrous membrane with fiber orientation varying among species (Packard and DeMarco, 1991). Depending on the species, eggs can be divided into one of two main categories: (1) flexible eggs with little to moderate mineral content and (2) rigid eggs with high mineral content (Packard and Packard, 1980). Figure 1 provides an overview of the following oviparous amniote eggshell characteristics. Among squamates (lizards and snakes) and archosaurs (crocodilians and birds),

the mineralized outer eggshell is mainly composed of calcium carbonate in the form of calcite, whereas in the chelonians (turtles, tortoises and terrapins) the eggshell is mainly in the form of aragonite, which is a less stable crystal polymorph of calcium carbonate (Packard et al., 1982). Tuatara are the sister lineage to squamates, but their flexible eggshell is a composite of calcite crystals embedded in the fibrous shell membrane (Cree et al., 1996).

Eggshell characteristics						
Flexible	+	+	+	+	-	-
Rigid	-	+	-	+	+	+
Calcite	-	+	+	-	+	+
Aragonite	-	-	-	+	-	-

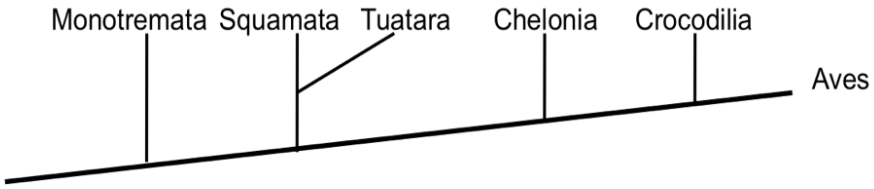

Figure 1. A character matrix comparing several eggshell characteristics of amniote groups over a cladogram depicting the evolutionary relationship of oviparous amniotes. Calcite and aragonite rows refer to the mineral state of calcium carbonate. A (+) symbol represents the characteristic is present in the oviparous amniote group and a (-) symbol represents the characteristic is absent. Depending on the species, some squamates and chelonians will lay flexible eggs while other species will lay rigid eggs.

Squamates deposit eggs with flexible eggshells that contain little or no mineral content with the exception of two subfamilies of geckos (*Sphaerodactylinae* and *Gekkoninae*) that lay eggs with rigid eggshells (Packard

and Packard, 1988). In eggs of the six-lined racerunner lizard (*Cnemidophorus sexlineatus*), the eggshell seems to lack an outer mineral layer of calcite (Trauth and Fagerberg, 1984). Similarly, the eggshell of the snake *Coluber constrictor* also lacks a thin crust, but it does contain nodular calcite crystals dispersed throughout the outer eggshell layer (Packard et al., 1982). The green anole, *Anolis carolinensis*, lays eggs that possess a thin outer calcareous layer composed of an open network of calcite spheres (Packard et al., 1982).

Depending on the species, chelonians lay eggs with varying degrees of mineralization, ranging from very flexible to rigid eggshells (Hirsch, 1983). The sea turtle, *Lepidochelys kempii,* deposits eggs with a thin calcareous layer. The shell unit that makes up the calcareous layer is described as a short and wide column that is slightly spaced from other units, allowing for some flexibility (Packard, 1999). The calcareous layer of the eggs of the snapping turtle, *Chelydra serpentine*, has shell units that are as wide as they are tall, and they are more closely arranged with some space in between groups of units (Hirsch, 1983). This arrangement of shell units makes the egg moderately flexible. The softshell turtle, *Trionyx spiniferus*, produces eggs that have rigid, heavily mineralized eggshells. The shell units are much taller than they are wide and closely adjacent to each other (Packard and DeMarco, 1991). Thus, eggshell flexibility or rigidity is dependent on how closely arranged shell units are to one another (Packard and Demarco, 1991).

All species of extant archosaurs (birds and crocodilians) lay rigid eggs with heavily mineralized eggshells (Packard, 1994). Bird eggshells have a highly conserved structure: a thin outermost non-calcified cuticle layer, a vertical crystal layer, the palisade layer, and the innermost mammillary layer immediately adjacent to the fibrous shell membrane. Each eggshell unit is a column with the palisade layer comprising the greatest portion of the eggshell thickness (Hincke et al., 2012). The tip of each mammilla is cone-shaped and is the site of calcium mobilization from the eggshell (Hincke et al., 2012). The mammillary layer is first formed from small organic cores within the fibrous shell membrane that then serve as nucleation sites for calcite crystal formation. The outgrowth of the crystals forms the shell units (Packard and DeMarco, 1991). Air-filled vesicles are found in the palisade layer and their numbers can vary depending on the species. Thicker shells, like those seen in the eggs of the ostrich, *Struthio camelus*, have smaller numbers of vesicles. In contrast, thinner shells like those of the parrot, *Agapornis roseicollis*, have a larger number of vesicles (Board and Sparks, 1991). Also, thin eggshells have single, uninterrupted pore canals, whereas thicker eggshells may have pore canals that fork (Board and Sparks, 1991).

The structure of crocodilian eggshells is similar to that of birds in that it also includes an outer compact mineral layer, a middle palisade layer, and an innermost mammillary layer. Marzola et al. (2014) provides a description of eggshell characteristics for three extant crocodilian species: American alligator

(*Alligator mississipiensis*), Philippine crocodile (*Crocodylus mindorensis*), and Cuvier's dwarf caiman (*Paleosuchus palpebrosus*). In the American alligator the eggshell is composed of wedge-shaped shell units. The surface layer of the eggshell is not smooth and is described as anastomotuberculate (wavy interconnecting ridges) followed by a compact crystal layer, a palisade layer, and a mammillary layer with conical tips. Vesicles are also present in the palisade layer as seen in bird eggshells (Ferguson, 1985). The shell units of the Philippine crocodile and Cuvier's dwarf caiman are wedge-shaped with a wider top than bottom. The surface layer of both species is not smooth and is described as rugosocavate (golf ball-like appearance) followed by a compact crystal layer, a palisade layer, and a mammillary layer with conical tips. The formation of the mammillary layer is similar to that of birds with an organic core serving as a nucleation site and crystals forming and radiating outward to make each eggshell unit (Packard and DeMarco, 1991).

Calcium Mobilization

It is clear that oviparous reptiles lay eggs with varying degrees of mineralization. However, reptilian eggs can be placed in one of two categories based on embryonic mode of calcium mobilization. Embryonic squamates rely mostly on yolk as their source of calcium, whereas chelonians and archosaurs main source of calcium derives from the eggshell (Packard, 1994). Embryonic lizards can sequester up to 60% of the calcium required for skeletal development from the yolk, and snakes can sequester more than 70% (Packard and Clark,

1996). In contrast, more than 70% of skeletal calcium derives from the eggshell in chelonians and archosaurs, with some archosaurs (such as the yellow-headed blackbird) mobilizing up to 90% of skeletal calcium from the eggshell (Packard and Clark, 1996).

The two sources of calcium the embryo can utilize for skeletal development come from the eggshell and yolk. The embryonic tissues responsible for mobilizing and transporting calcium are the chorioallantoic membrane (CAM) and yolk sac membrane (Packard and Packard, 1984). The current model for transcellular calcium transport involves calcium channels on the apical surface, a calcium binding protein in the cytosol, and plasma membrane calcium ATPase (PMCA) on the basolateral surface (Hoenderop et al., 2005). Original work on calcium transport via the CAM or yolk sac was done mostly on embryonic birds, primarily galliform species (Tuan et al., 1991). Eggshell calcium is first solubilized by the enzymatic action of carbonic anhydrase, which acidifies the calcite in the mammillary tip. Carbonic anhydrase is primarily located in the villus cavity cells, one of two common chorionic cell types. Free calcium is bound to an apical calcium binding protein (transcalcin), and then absorbed via pinocytosis. The concentration of calcium inside the endosome is increased via the action of a PMCA imbedded in the endosome. As the endosome travels across the cell it is acidified internally which unbinds calcium from transcalcin. Eventually, the calcium rich vesicle fuses with the basolateral membrane and releases the calcium into the serosal space. The

calcium then enters the blood vessels, and is transported (presumably bound to a carrier protein) to the embryo and/or yolk sac (Tuan et al., 1991).

It has been shown in chicken eggs that calcium is stored in the yolk in the form of spherocrystals composed of multilayered lecithin liposomes with vaterite crystals (a polymorph of $CaCO_3$) in between the layers (Tong et. al, 2008). The exact mechanism for how calcium is mobilized by the yolk sac is not known. However, it is believed that the yolk sac endothelial cells absorb yolk via phagocytosis (Packard and Clark, 1996). Histological cross sections of embryonic chicken yolk sacs have shown vacuoles containing yolk material in endodermal epithelial cells (Tuan et al., 1991). The yolk material in the vacuoles is then digested and the contents are released into the vitelline circulation. It has been shown in bird embryos that yolk calcium mobilization is regulated by vitamin D_3, which promotes the expression of a calcium binding protein (calbindin D_{28K}). Calbindin D_{28K} is found in the yolk sac endodermal cells and is believed to assist in transcellular transport of calcium (Tuan et al., 1991). Although calcium mobilization studies focused on bird embryos, the process of calcium mobilization is believed be similar in non-avian embryonic reptiles. For instance, calbindin D_{28K} expression has been shown in CAM and yolk sac epithelial cells in the corn snake, *Elaphe guttata* (Ecay et al., 2004), as well as in the reproductively bimodal viviparous lizard *Zootoca* (former *Lacerta*) *vivipara* (Stewart et al., 2011). This suggests that calbindin D_{28K} has been evolutionarily

conserved only in bird yolk sac endodermal cells, and transcalcin (found in the CAM) may possibly be unique to archosaurs.

One way to categorize eggs of oviparous reptiles can be based on how embryos mobilize and utilize calcium. Packard (1994) reviewed the mode of calcium mobilization among oviparous reptiles. During incubation, squamates mobilize calcium from the yolk and virtually deplete it of calcium by the time they hatch, at which time they are entirely reliant on their diet for their calcium supply. The same pattern is observed among chelonians, despite notable differences in eggshell structure among clades (Packard and Packard, 1991). Archosaurs, however, mobilize egg calcium reserves in a different manner. During the differentiation phase, embryos mobilize calcium from the yolk. During growth phase, eggshell calcium is mobilized and yolk calcium stores are replenished (Packard and Packard, 1989). Thus, archosaur hatchlings have residual yolk with enough calcium that they are not initially reliant on their diet for their calcium needs. For example, it has been estimated that hatchling alligators can potentially rely on the energy stores in the residual yolk sac and body fats for more than four months (Fischer et al., 1991). Presumably, hatchlings can utilize the calcium stored in the residual yolk sac if prey are not available.

Aims

Packard and Seymour (1997) suggested that embryos from early oviparous reptiles that could not utilize the eggshell as a source of calcium would have hatched in a diminutive state compared to those that could have used the

eggshell. To date, no study has looked at the effects of removing the eggshell as a source of calcium in archosaur eggs. How the removal of the calcareous eggshell layer may affect embryonic skeletal development is not known. Therefore, this study aims to address the following questions:

- Does removal of the calcareous eggshell layer reduce embryonic growth?
- Does loss of eggshell calcium supply affect the onset of bone mineralization in embryos?
- Does calcium mobilization occur evenly across the inner surface of the eggshell?
- Do experimental hatchlings show compensatory growth?
- Are maximum bite forces similar between experimental and control hatchlings?
- Does eggshell removal affect cross-sectional geometric properties of the hatchling skeleton?

To address these questions experimentally, I used eggs, embryos and hatchlings of the American alligator (*Alligator mississipiensis* Daudin 1801) as a non-traditional animal model.

Animal Model

Prior studies on shell-less chicken egg cultures techniques have been done, however there are some drawbacks to this approach. First, the removal of the fibrous shell membrane requires cultures to be incubated in a sterile environment with increased humidity to minimize evaporative water loss. Second,

embryos must be rocked to redistribute fluids in the egg compartments and help promote embryonic growth. Third, mineral supplementation must be provided to help improve embryonic survivability (Dunn, 1991). Despite being of similar egg mass (55g for chicken and up to 70g in alligators), alligator eggs have a much thicker eggshell (~0.5mm) than chicken eggs (0.3-0.4mm) (Marzola et al., 2014; Hincke et al., 2012), and their wedge-shaped shell unit allows for less packed mammillary tips attached to the fibrous membrane compared to the more tightly packed tubular shell unit of the chicken egg. Alligator eggshells should be easier to physically peel by hand, which means a lower risk of rupturing the fibrous shell membrane and infecting the egg during experimental treatment. Also, alligator eggs do not need to be turned as do bird eggs. Furthermore, alligator embryos do not start to mobilize eggshell-bound calcium until around day 50 of incubation (Packard and Packard, 1989). This provides sufficient time to manually remove the entire eggshell before the embryo can begin to utilize it as a source of calcium for skeletal development.

Hypotheses

H1: Removal of the calcareous eggshell layer during early stage of development (Ferguson stage 15) will reduce embryonic growth rate and produce diminutive hatchlings.

H2: Removal of the calcareous eggshell layer will affect onset of bone mineralization in embryos.

H3: The eggshells of control specimens will have a decreasing but uniform thickness throughout the eggshell during incubation.

H4: Experimental hatchlings will display compensatory growth with control hatchlings.

H5: Voluntary maximal bite force of experimental hatchlings will be lower than that of similarly-sized control hatchlings.

H6: Experimental hatchlings will have a reduced bone cross-sectional area, second moment of area, and polar moment of inertia in both the mandible and femur.

CHAPTER TWO

MATERIALS AND METHODS

Acquisition of Eggs and Care

Alligator eggs were acquired from the Rockefeller Wildlife Refuge in Grand Chenier, Louisiana. The dorsal side of each egg was longitudinally marked with a pencil, which indicated the correct orientation of the egg. Placing the egg in a different orientation can potentially kill the embryo. Clutches were placed in a large cooler, arranged in columns in damp Vermiculite™ and transported overnight via van to California State University San Bernardino (CSUSB). Immediately upon arrival at CSUSB, each clutch was wiped clean with a moist paper towel, transferred to a plastic container filled with Vermiculite™, and placed in constant temperature cabinet (BINDER APT.line™ KBW model E5.1, Tuttlingen, Germany). Incubation temperature was set to 30˚C (following methods of Owerkowicz et al., 2009), so as to ensure female embryos due to temperature-dependent sex determination (Deeming and Ferguson, 1989). Trays filled with water were also placed in the incubator to keep the relative humidity at 100%. Eggs were sprayed as needed with tepid water, to maintain water potential of the incubating chambers. Egg viability was checked regularly (see below) and any dead eggs (assessed by smell, retraction of the CAM, and egg discoloration) were removed from the container.

Experimental Setup and Sampling

Experimental eggs had their calcareous eggshell physically peeled by hand, while control eggs were sham-handled but otherwise not altered. Using a pair of flat-tipped forceps, a small crack was made near one of the egg's poles and from there the calcareous shell was flaked off in small pieces. Whenever the fibrous shell was punctured during the peeling process, a small piece of the calcareous shell was superglued to the punctured site. If the puncture was large and could not be sealed, the egg was discarded. At time 0 (time of peeling), embryonic developmental stage was back-calculated from staged control embryos collected during early sampling periods. Initial embryonic stage was determined to be stage 15 following the criteria established by Ferguson (1985).

For both experimental and control eggs, the edge of the CAM was marked on the eggshell and shell membrane with a pencil. Areas where the CAM underlies the fibrous shell membrane appeared white, whereas where it did not would appear grey in color (See Figure 2). These markings served as a visual reference of the embryo's viability. If the embryo was alive, then the CAM advanced toward the poles past the initial pencil marks. If the embryo was dead, however, the CAM did not advance toward the poles past its initial labeled marks, and sometimes even retracted toward the equator.

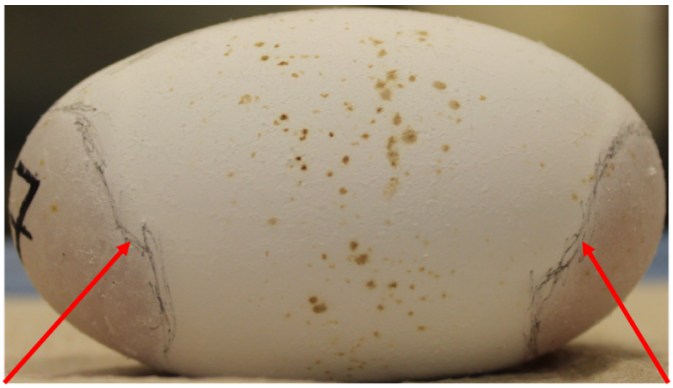

Figure 2. Photograph of a peeled experimental egg. Red arrows are pointing to the edge (outlined with pencil) of the CAM. Areas where the CAM has spread will appear white, while areas without the CAM will appear grey in color.

Sampling of specimens occurred at weekly intervals, starting on the initial week of the shelling process and continuing until hatching. Embryos *in ovo* were anesthetized with Isoflurane™ for several minutes before embryos were removed. Experimental (n=6) and control (n=6) eggs were opened with a pair of scissors, so as to remove the dorsal half of the eggshell. The embryo and the yolk sac were carefully dissected out, lightly blotted with tissue paper, and their respective wet masses recorded (±0.1mg) on an analytical balance (OHAUS® Model No. AP110-0 Plus). Early stage embryos were quickly preserved in 10% neutral buffered formalin (NBF) while later stage (stage 20+) had their limb and tail skin incised longitudinally to allow for better infusion of NBF during fixation. Yolk sacs were placed in a 70°C drying oven for three days, or until their dry mass had ceased to decrease. They were stored in 50ml Falcon tubes at -20°C

until they were ready for ashing in a muffle furnace. The top and bottom halves of eggshells from control eggs were rinsed under tap water, blotted lightly with a paper towel, and air-dried, while the fibrous shell membrane of experimental eggs was discarded.

Ashing

Dried yolk sacs were placed in aluminum weighing boats and ashed in a muffle furnace (Barnstead Thermolyne 1400) at 600°C for three days. Dry mineral ash was weighed on the analytical balance (OHAUS® Model No. AP110-0 Plus).

Eggshell Measurements

The eggshell from control eggs was carefully removed with fine tipped forceps from the fibrous membrane. Eggshell thickness was measured with a dial caliper gauge (Mitutoyo 209-406, ±0.01mm scale interval) at six locations: both poles, and four sides around the equator (dorsal, ventral, and two lateral). Each region was labeled with a dotted pattern (Figure 3) before measuring so to avoid sampling the same area. A total of six measurements were taken from each region, and were then averaged.

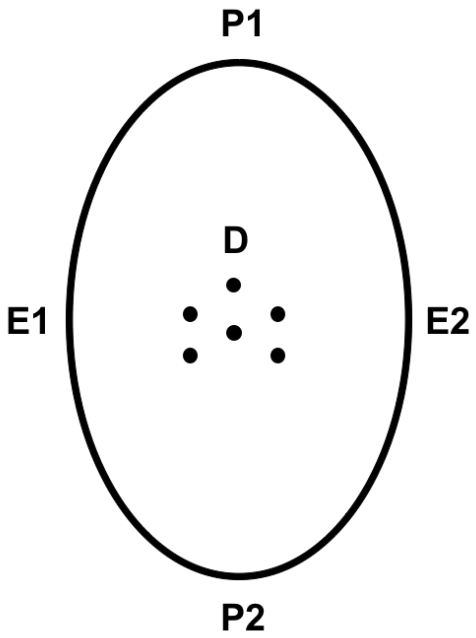

Figure 3. Schematic drawing of an alligator egg. Letters represent sampling areas around the egg with “D” depicting the dorsal side of the egg. The six measurements per sampling region are represented by the black dots (made with a black Sharpie® marker) arranged in a pentagonal pattern with the sixth dot in the middle.

Post-hatching Sampling

Some of the eggs (from three different clutches) in each treatment group (n=22 control and n=27 experimental) were incubated until hatching. Hatchlings had their growth monitored for two months. Each week the following measurements were taken: head length, head width, snout-vent length, and total

body length (after Deeming and Ferguson, 1989). Each treatment group was placed in separate plastic containers (n=10) and housed in the university vivarium. All treatment groups were fed gator chow (Lone Star® 50% alligator food with 3.25% calcium) twice a week.

Bite-force Testing

Voluntary bilateral bite force was also measured in three months-old hatchlings using a custom-built double-cantilever beam force transducer with steel bite plates built around a piezoelectric isometric force transducer (type 9203, Kistler, Switzerland) connected to a charge amplifier (type 5595, Kistler, Switzerland). The metal biting surfaces of the plates were covered with thin leather strips to protect the animal's teeth and provide a naturalistic surface to encourage high-effort biting. See Lappin and Jones (2014) for detailed information on the apparatus, its preparation for trials, and calibration. For each hatchling, the maximum voluntary bilateral bite force was measured in triplicate within a span of three minutes, and the maximum force was recorded. Core body temperature was 30±1°C, confirmed with a cloacal thermocouple. Additionally, hatchlings were video recorded (at 30 fps) using a Cannon EOS Rebel T3i digital camera. Using Image J (version 1.50e), still frames from the recordings were used to measure the lever arm distance between the quadratoangular jaw joint and the point of contact on the lower plate. Bite torque was calculated as a product of maximum bite force and lever arm.

Clearing and Staining

To determine the onset of mineralization of individual skeletal elements, embryonic specimens underwent a clearing and staining process with alizarin red and alcian blue. The following protocol was adapted from Song et al. (1995), Wassersug (1976) and Vickaryous and McLean (2011), with time per solution dependent on specimen size.

Depending on the developmental stage, specimens were skinned post-cranially and eviscerated. Embryos from stage 23 and below were not skinned, but stage 24+ embryos and hatchlings were skinned to allow for better cartilage staining. Paraxial skin tracts on the dorsal aspect of the specimen, which later in ontogeny develop osteoderms (Seidel, 1979), were left intact. Table 1 summarizes the amount of time each specimen spent in a solution during each step. After skinning, the specimens were washed in de-ionised water (de-I H_2O) in order to remove formalin. Next, specimens were dehydrated using ethanol (EtOH) solutions of increasing concentration. Embryos were placed in 70%, 95%, 100% and then another 100% EtOH.

After dehydration, specimens were placed in an Alcian Blue solution to stain for cartilage. Each solution was made with 160ml of 100% ethanol, 40ml of glacial acetic acid and 20mg of Alcian Blue 8GX. Embryos were then placed in a 100% ethanol solution to fix the cartilage staining. Afterwards, specimens underwent rehydration using a series of EtOH solution of decreasing concentration (70%, 50%, 25% EtOH), and finally 100% de-I H_2O.

Table 1. Summary of clearing and staining steps with the amount of time specimens will spend in each solution.

Step	Time	
	Early (stage 21-)	Late (stage 22+)
Washing	1 hour per wash	overnight
Dehydration	1 hour per wash	1-2 days
Cartilage staining	overnight	2-3 days
Cartilage fixation	overnight	2-3 days
Rehydration	2 hours per wash	2 days
Neutralization	overnight	2-3 days
Bleaching	overnight	3-5 days
Tissue digestion	1-2 hours	2-5 days
Bone staining	overnight	2-3 days
Clearing	1 day per solution	2-4 days per solution

After rehydration, specimens were placed in a saturated solution of sodium borate to prevent the loss of calcium during the bleaching process. Next, each bleaching solution contained 250ml of 0.5%KOH with 5 drops of 30% H_2O_2 added daily until the specimen was bleached. Extent of bleaching was assessed visually by the lightening of cranial and dorsal dark skin pigment. Specimens were then transferred into a trypsin solution for muscle digestion. Each solution was made with 60ml of saturated sodium borate, 140ml of de-I H_2O, and 2g of trypsin powder. Depending on the duration of muscle digestion, solutions were changed every two days until bones were clearly visible.

After trypsin digestion, specimens were placed in an alizarin red S solution to stain the bones. 50mg of alizarin red S powder was added to a 200ml solution of 0.5% KOH. Specimens were next transferred into a series of 0.5%KOH/glycerin 200ml clearing solutions. Embryos were transferred into a 3:1,

2:1, 1:1, 2:1, and 3:1 KOH/glycerin solution. Finally, specimens were stored in 100% glycerin and imaged with a Cannon EOS Rebel T3i digital camera. The first appearance of the alizarin stain in individual cranial and post-cranial bones was recorded as indicative of ossification.

Further, the humerus and the femur were imaged in lateral view at higher magnification. Their total lengths were measured in Image J (version 1.50e). The extent of ossification (stained with alizarin red S) was expressed as % of total bone length.

Bone Histology

The left femur and the lower jaw of hatchlings were excised and dehydrated in a series (70-100%) of EtOH solutions. Specimens were then vacuum-pumped at -635 mmHg for two hours to allow proper infusion of ethanol. After dehydration, the femora and jaws were air-dried overnight and embedded in epoxy (Epo-Tek® type 301, Epoxy Technology, Inc., Billerica, MA) and osteobed (Osteo-Bed Resin Solution A, Polysciences, Inc., Warrington, PA), respectively. Following polymerisation, three 1mm- thick serial sections were taken from the femoral midshaft on a low speed saw (Buehler IsoMet® Low Speed Saw). Three 1mm-thick section were also taken from the caniniform tooth bearing region of the mandibular ramus. Sections were mounted on slides with epoxy, ground to approximately 100 µm thickness on a grinder-polisher (Buehler Metaserv® 3000 variable speed) and coverslipped with Permount™. Slides were imaged under a zoom stereomicroscope (Nikon SMZ800) at 35-63x magnification. Non-osseous

tissue, including the marrow, periosteum, as well as any teeth, Meckel's cartilage and mandibular nerve (in the lower jaw), was digitally removed in Adobe Photoshop CS6. Femoral cross-sections were orientated by using pre-marked dorsal and medial-anterior regions. Jaw cross-sections were orientated by placing the two dorsal edges of the tooth socket level. The cross-sectional area (CSA) of bone was measured and second moment of area (*Ix*), and polar moment of inertia (*J*), calculated using ImageJ software with MomentMacroJ v1.4B plugin.

Data Analysis and Statistics

To assess whether there was an effect of experimental eggshell removal treatment on body mass and yolk mass, a one-way analysis of variance (ANOVA) was conducted for each independent time point. An ANOVA was conducted for each independent time point for all growth trajectories. An ANOVA was conducted on each independent time point for ash content. Eggshell thickness was tested with an ANOVA for each independent time point and a Tukey-Kramer HSD post-hoc was used to test for differences between regions. Femur and jaw cortical bone thickness were compared between experimental and control embryos/hatchling's with a ANOVA. An analysis of covariance (ANCOVA), with treatment group as factor and individual bone length as covariate, was used to test for differences in geometric properties (e.g. *I* and J) of the femur and the lower jaw. Difference in mean lacunar density between experimental and control hatchlings was tested with a Wilcoxon ranked sums

test. A power regression line was used to best describe embryonic growth and a second-order polynomial regression line was used to best describe a decrease in yolk wet mass and ash mineral mass. A linear regression line was used for all other variables. A p-value of 0.05 was chosen to detect significance.

CHAPTER THREE

RESULTS

Embryo and Yolk Measurements

2012 Season

During the first seven days post-shelling (Ferguson stage 19), embryo wet mass was similar between both groups (Figure 4a). At 14 days (Ferguson stage 21), however, experimental embryos were 13% smaller than control embryos (ANOVA, $F_{1,10}$=8.177 P<0.01). The difference in wet mass continued to widen throughout incubation. At hatching, experimental alligators were 42% smaller than their control siblings (ANOVA, $F_{1,27}$=79.526, P<0.0001, Figure 4a and Figure 5). Yolk sac wet mass was similar between both groups for the first 35 days post-shelling (Figure 4b). At 42 days (Ferguson early stage 28), yolk sacs of experimental embryos were 36% heavier than control yolk sacs (ANOVA, $F_{1,10}$=20.751, P<0.001). The difference in wet mass continued to widen until hatching. At hatching, yolk sacs of experimental animals were 113% heavier than yolk sacs of control hatchlings (ANOVA, $F_{1,27}$=26.597, P<0.0001).

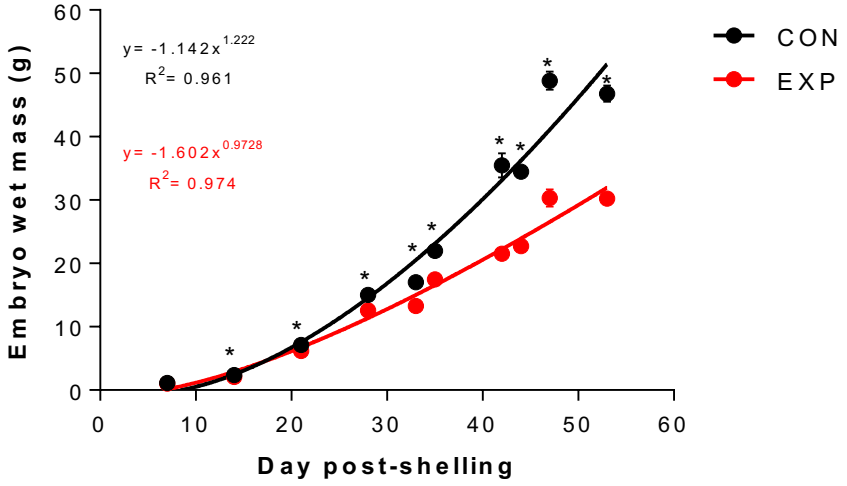

A

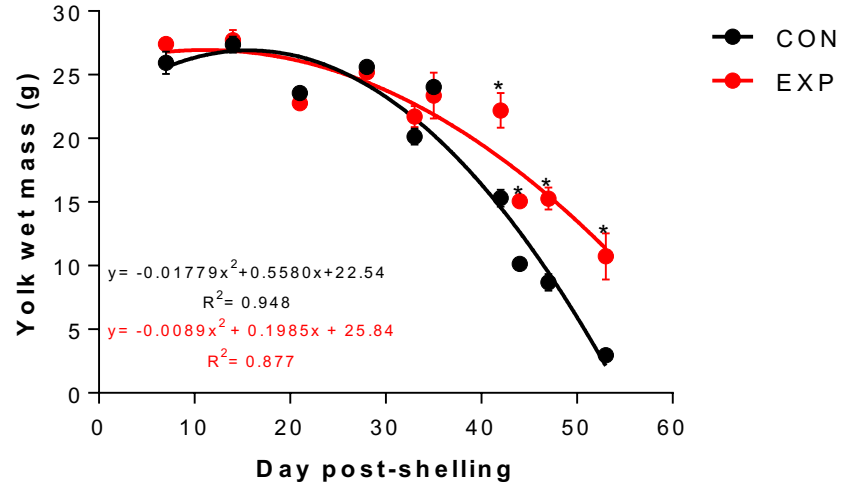

B

Figure 4. Graph of alligator embryonic wet mass (A and C) and yolk wet mass (B and D) against time. Black symbols represent data from control eggs (with eggshell intact), and red symbols represent data from experimental eggs (with eggshell removed). Time 0 is the day of eggshell removal. Each pair of time points represents an average of eggs (n=6) from the same clutch; asterisks represent a significant difference (ANOVA, $p<0.05$). Different time points report data from different clutches. Least-square regression lines are based on power equations for embryo wet mass and second order polynomial equations for yolk wet mass.

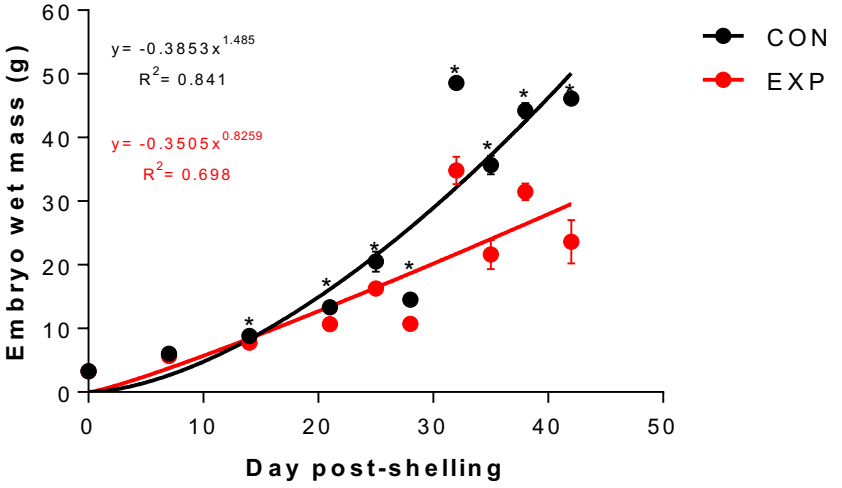

C

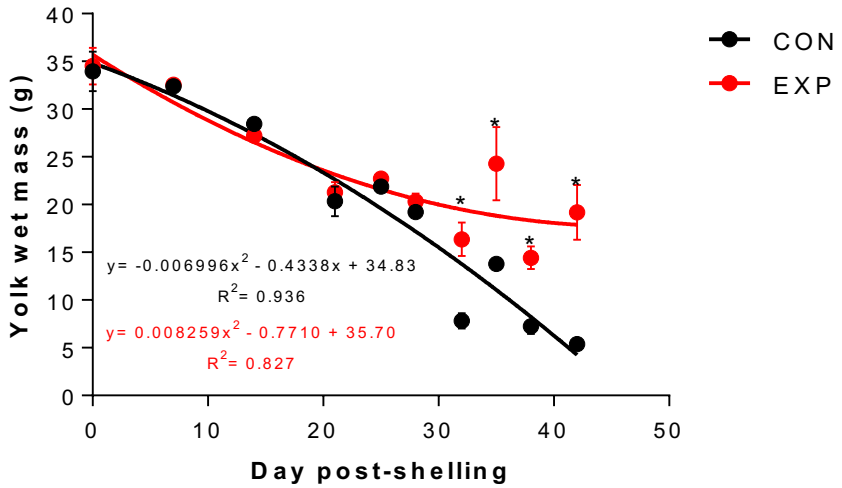

D

Figure 4. (continued) Panels A and B are based on data from eggs collected in summer 2012, and panels C and D are from summer 2013. Significant difference in embryo wet mass is observed on day 14 and continues to increase throughout incubation (A, C). Control embryos grew at a faster rate than experimental embryos. B) Significant differences in yolk wet mass appear at day 35 (B) or 32 (D) post-shelling, and continue to increase until hatching, control yolk sacs are significantly lighter than experimental.

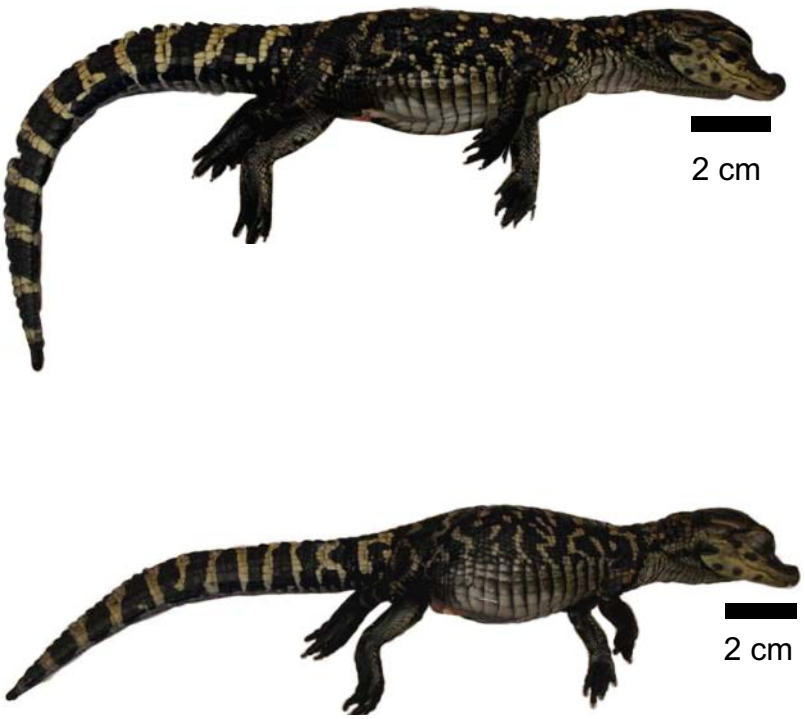

Figure 5. Lateral view of representative hatchlings from the control (top) and experimental (bottom) groups. Both animals are clutched-matched siblings.

At seven days post-shelling, total body lengths of experimental embryos were similar to control embryos (Figure 6a). However, at 14 days post-shelling experimental embryos were 6% shorter than control embryos (ANOVA, $F_{1,10}$=25.589, P<0.001). At hatching, experimental animals were 13% shorter than control animals (ANOVA, $F_{1,20}$=35.143, P<0.0001). At seven days post-shelling, the snout-vent lengths of experimental embryos were 6% shorter than

control embryos (ANOVA, $F_{1,10}$=7.629, P<0.05; Figure 6b). At hatching, the snout-vent length of experimental animals was 15% shorter than control animals (ANOVA, $F_{1,20}$=76.181, P<0.0001). At seven days post-shelling, the head length of experimental embryos was 8% shorter than control embryos (ANOVA, $F_{1,10}$=16.653, P<0.05; Figure 6c). At hatching, the head length of experimental animals was 11% shorter than control animals (ANOVA, $F_{1,20}$=59.227, P<0.001). At seven days post-shelling, the head width of experimental embryos was similar to control embryos. However, at 14 days post-shelling experimental embryos were 4% shorter than control embryos (ANOVA, $F_{1,10}$=13.234, P<0.01; Figure 6d). At hatching, the head width of experimental animals was 17% shorter than control animals (ANOVA, $F_{1,20}$=13.067, P<0.001).

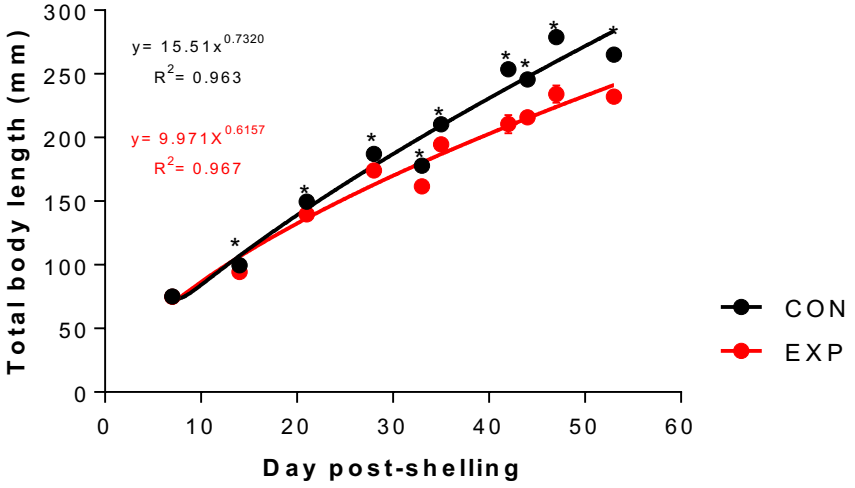

A

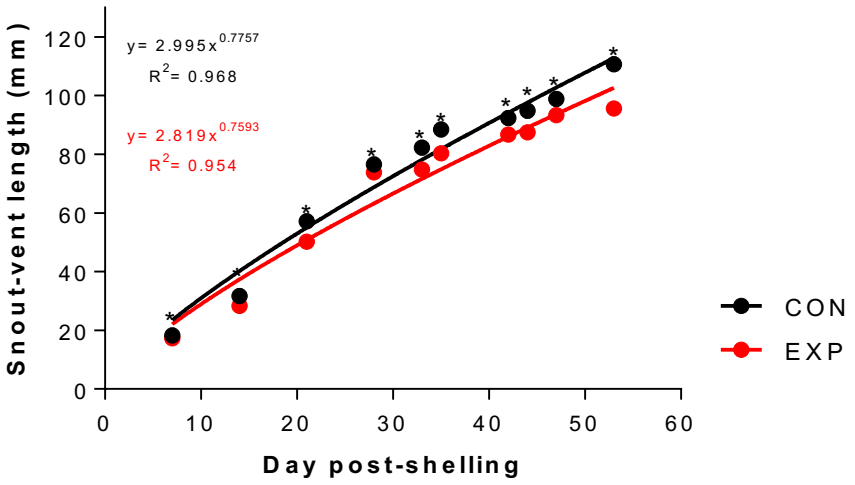

B

Figure 6: Graph of alligator embryonic growth trajectories during incubation (A-D). Least-square regression lines are based power regression equations. Black symbols represent data from control eggs (with eggshell intact), and red symbols represent data from experimental eggs (with eggshell removed). Each pair of time points represents an average of eggs (n=6) from the same clutch; asterisks represents a significant difference (ANOVA, $p<0.05$). Different time points report data from different clutches.

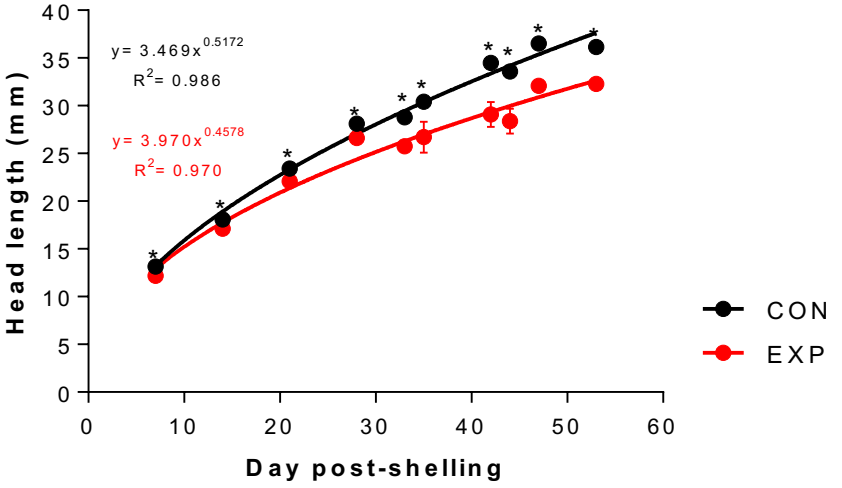

C

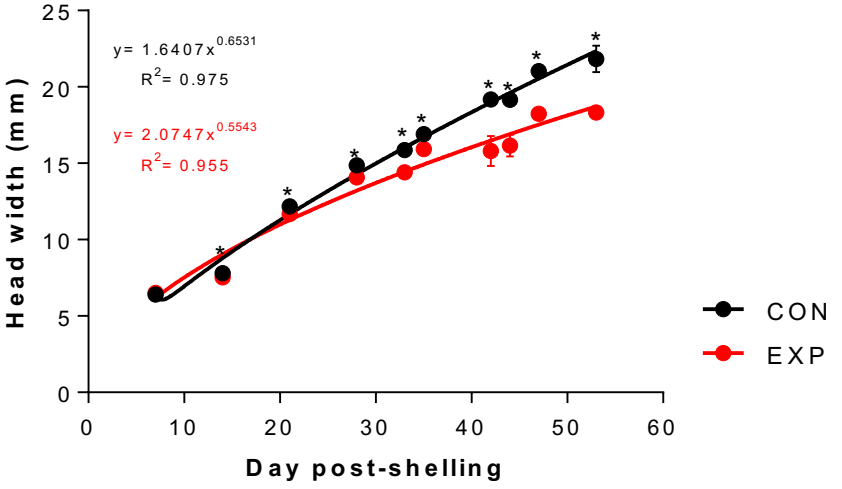

D

Figure 6 (continued). All panels are based on data from eggs collected in summer 2012. A and C) No initial difference in growth was observed at 7 days post-shelling. Significant difference was first observed 14 days and persisted up to hatching. B and C) Significant difference was first observed at 7 days post-shelling and persisted until hatching.

2013 Season

Eggs collected in the summer of 2013 were slightly older in development than those collected in the summer of 2012, however, the repeat experiment

yielded similar results. For the first week post shelling (Ferguson early stage 22), embryos showed no difference in wet mass (Figure 4c). At 14 days post-shelling (Ferguson late stage 24) experimental embryos were 13% lighter (ANOVA, $F_{1,10}$=11.983, P<0.01). The difference in wet mass continued to increase throughout incubation with experimental animals being 64% lighter than control animals at hatching (ANOVA, $F_{1,9}$=52.419, P<0.0001). At 28 days post-shelling, there was no difference in yolk sac wet mass (Figure 4d). However, at 32 days post-shelling (Ferguson late stage 27) experimental yolk sac wet mass was 70% greater than control yolk sacs (ANOVA, $F_{1,10}$=19.579, P<0.001). The difference in yolk wet mass continued to increase until hatching. At hatching, experimental animals had yolk sacs that averaged 112% heavier than those of control animals (ANOVA, $F_{1,9}$=26.390, P<0.001).

Eggshell Thickness

Measurements of control eggshells taken at time 0 of the experiment showed a significant difference (ANOVA, $F_{3,8}$=11.553, P<0.01) in thickness among polar and equatorial regions (dorsal, ventral, and lateral), and that the poles were significantly thinner than the equator (Tukey-Kramer HSD, P<0.05). At time 0 (time of shelling), poles were 14% thinner than the equatorial regions (Figure 7). However, there was no significant difference among the equatorial regions. At hatching, poles were 26% thinner than the equator (ANOVA, $F_{3,32}$=10.966, P<0.0001). Overall, there was a general decrease in eggshell thickness throughout incubation with the poles being consistently and

significantly thinner (Tukey-Kramer HSD post hoc test, $P<0.05$) than the equator (Figure 7).

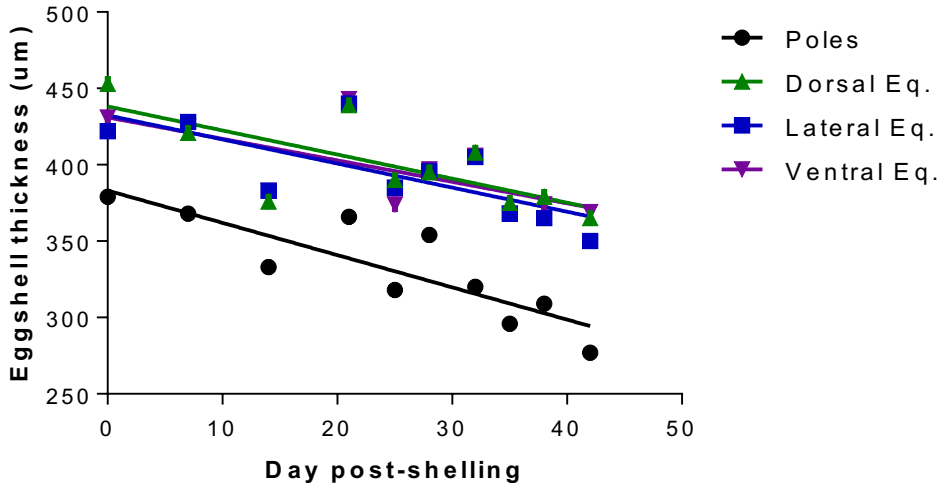

Figure 7. Changes in eggshell thickness from the polar and equatorial regions of the control eggs during incubation. At each time point, data represent average (n=6) values from the same clutch; different time points sample are from different clutches. Note that eggshell at the poles is significantly thinner than at the equator (ANOVA, $p<0.05$). There are no significant differences between three equatorial sites (ventral, lateral and dorsal). Further, eggshell thickness shows a steady decrease with duration of incubation at all sites (ANCOVA, $p<0.05$). Linear regression equation: $y= -2.113x +383.1$, $R^2= 0.732$ (Poles); $y=-1.575x + 438.2$, $R^2= 0.537$ (Dorsal Eq.); $y= -1.578x + 432.4$, $R^2= 0.538$ (Lateral Eq.); $y= -1.407x + 431.1$, $R^2= 0.478$ (Ventral Eq.).

Yolk Ash Mineral Content

From seven to 35 days post-shelling, there was no difference in yolk ash mineral mass between treatment groups (Figure 8). However, a significant difference (ANOVA, $F_{1,7}$ =6.681, $P< 0.05$) was first observed from samples taken

on day 42 post-shelling. Yolk sacs from experimental eggs contained 37% more mineral ash than that from the control eggs. This difference in mass continued up until hatching. At hatching, yolk sacs from experimental eggs contained 70% more mineral ash than that from the control eggs. Plotting ash mineral mass against dry yolk mass showed that ash mineral mass decreased with lower dry yolk mass (Figure 9). Dry yolk from experimental eggs had similar ash mineral mass compared to control eggs sampled between Ferguson stage 19 and late stage 25. From Ferguson stage 27 until hatching, however, dry yolk from experimental eggs had lower ash mineral mass than that from control eggs.

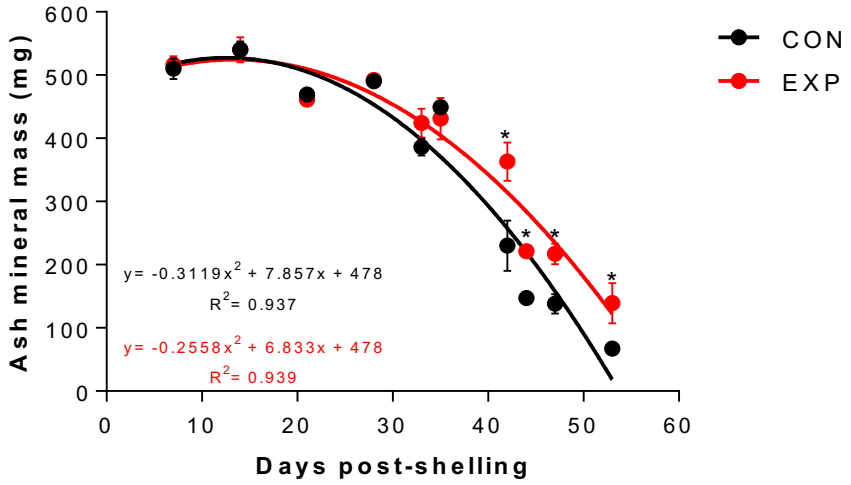

Figure 8. Dry mass of ash mineral from yolk sacs from alligator embryos (2012 season) against incubation time (post-shelling). Black symbols represent data from control animals and red symbols represent data from experimental animals. Least-square regression lines are based on second order polynomial equations. Each pair of time points represents an average of ashed yolk sacs (n=6) from the same clutch. An asterisk represents a significant

difference (ANOVA, $p<0.05$). A significant difference is first observed at 42 days post-shelling, with experimental yolks sacs containing greater mass mineral, and increasing toward time of hatching (56 days).

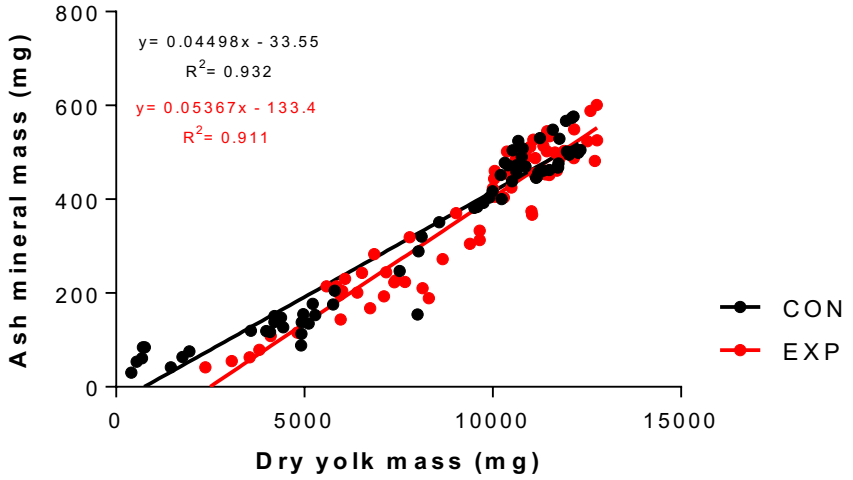

Figure 9. Graph of dry mass ash plotted against dry yolk with added linear regressions. Black symbols represent data from control animals and red symbols represent data from experimental animals. Data points from the upper right hand region of the graph represent yolk taken at early incubation. Data points from the lower left hand region represent yolk taken during late incubation and hatching. There is a significant difference (ANCOVA, $p<0.0001$) for amount of ash mineral over dry yolk between experimental and control yolk ash as represented in the lower left-hand corner.

Progression of Skeletal Mineralization

No visible mineralization of bone (stained with alizarin red S) was observed at seven days post-shelling (Ferguson stage 19) in either experimental or control embryos (Figure 10a and 10b). At 14 days post-shelling (Ferguson

stage 21), parts of the cranium and lower jaw began to mineralize in both experimental and control embryos (See Table 2 for the list of visibly ossified bones). In addition, the mid-shafts of the long bones of the limbs began to mineralize (Figure 10c and 10d). At 21 days post-shelling (Ferguson stage 23), the mineralization of the cranium continued to proceed along with both jaws. Teeth were now mineralized in both experimental and control embryos. At this stage the vertebral column, specifically the centra, began to mineralize except for the distal caudal vertebrae (Figure 10e and 10f). Mineralization of the pectoral girdle, pelvic girdle, ribs, metacarpals, and metatarsals had also commenced. Furthermore, by day 21, gastralia had appeared in both experimental and control embryos.

At 28 days post-shelling (Ferguson late stage 24), most of the caudal vertebral centra had been mineralized. Neural spines in the cervical region also began to mineralize but were not observed in other regions of the vertebral column. Mineralization of the phalanges (manual and pedal) began in both experimental and control embryos (Figure 10g and 10h). At 33 days post-shelling (Ferguson early stage 25), the vertebral zygapophyses began to mineralize in the thoracic region. The radiale and ulnare were now visible in both experimental and control embryos (Figure 10i and 10j). At 35 days post-shelling (Ferguson late stage 25), the thoracic transverse processes began to mineralize along with the lumbar zygapopheses. The calcaneum was also visible in both experimental and control embryos (Figure 10k and 10l).

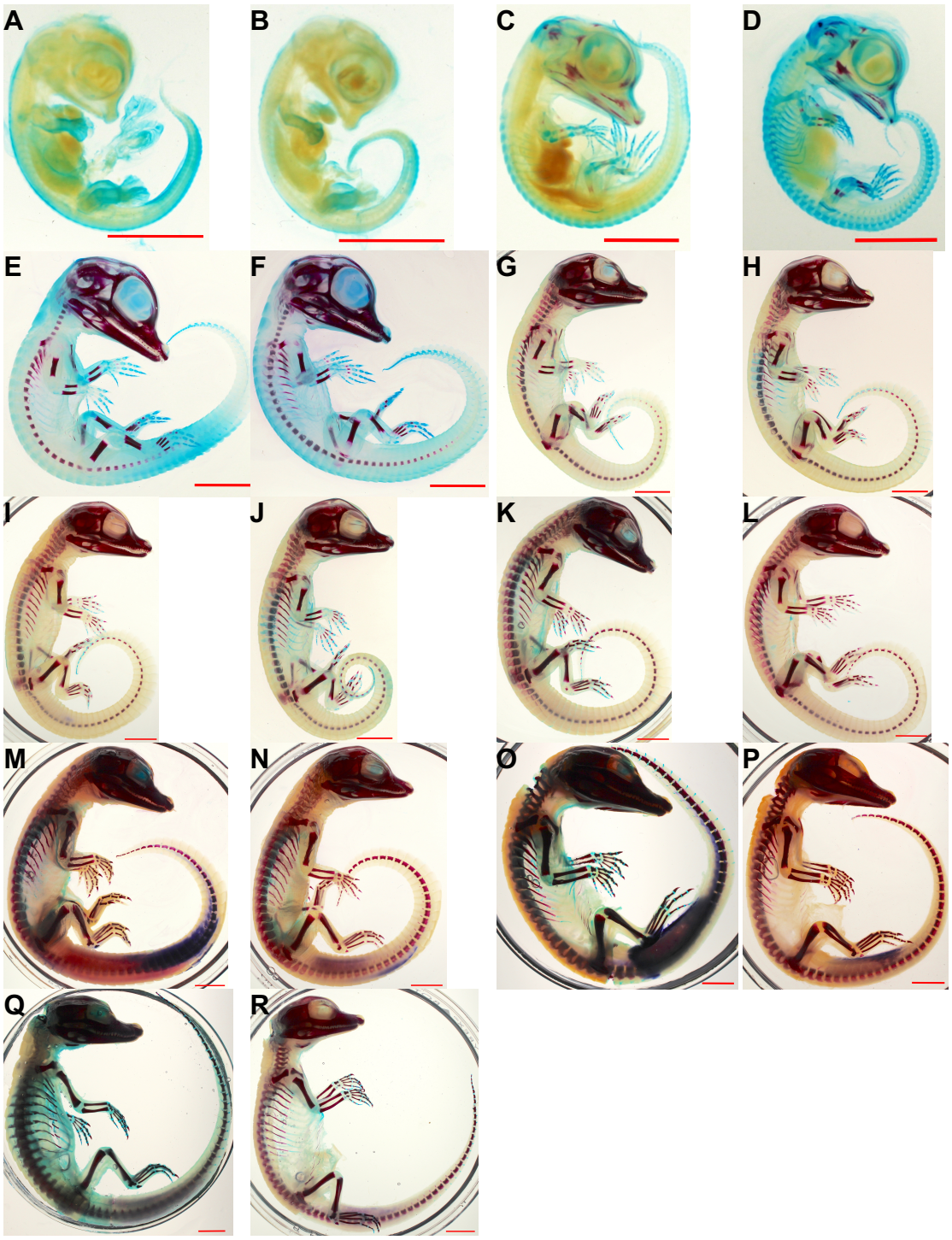

Figure 10. Photographs of cleared and stained embryos from the 2012 season. Panels A, C, E, G, I, K, M, O, and Q are control animals. Panels B, D, F, H, J, L, N, P, and R show experimental animals. Bone was stained red and cartilage was stained blue. Embryos from panels A and B are at stage 19. Embryos from

panels C and D are at stage 21. Embryos from panels E and F are at stage 23. Embryos from panels G and H are at late stage 24. Embryos from panels I and J are at early stage 25. Embryos from panels K and L are at late stage 25. Embryos from panels M and N are at stage 27. Embryos from panels O and P are at late stage 28. Panels Q and R show hatchlings. All red scale bars are 10mm long. Note that bone does not begin to mineralize until stage 21. From stage 21 onwards, time of bone mineralization in experimental embryos is the same as for control embryos.

Table 2. Table describing the embryological stage during which different mineralized bones were observed. Time of bone mineralization in experimental animals was the same as for control animals (see Fig. 10 for visual comparison). The appearance of carpalia (wrist bones) was only observed in control hatchlings and not in experimental hatchlings.

Embryonic Stage	Mineralized Bone		
19	None		
21	angular dentary femur fibula frontal humerus	jugal maxilla oticcapsule postorbital prefrontal premaxilla	pterygoid radius splenial surangular tibia ulna
23	basi-occipital caudal centrum cervical centrum coracoid gastralia hyoid ilium interclavical ishium	lacrimal lumbar centrum metacarpal metatarsal nasal parietal phalange (pes) quadrate quadratojugal	ribs scapula squamosal sternum teeth temporal thoracic centrum
Late 24	cervical neural spine cervical ribs		phalange (manus) pubis
Early 25	radiale thoracic zygapophyses		ulnare
Late 25	calcaneum lumbar zygapophyses	thoracic transverse process	
27	astragalus caudal chevron caudal zygapophyses	lumbar neural spine thoracic neural spine	 pisiforme
Late 28	caudal neural spine		
Hatchling	carpalia (only in controls)		

At 44 days post-shelling (Ferguson stage 27) the last remaining caudal vertebral centra had finished mineralizing. The thoracic and lumbar neural spines and caudal zygapophyses were now visible. Caudal chevrons also began to appear in the first half of the tail. Additionally, the pisiforme and astragalus were now visible in the manus and pes of both experimental and control embryos, respectively (Figure 10m and 10n). At 47 days post-shelling (Ferguson late stage 28) caudal neural spines began to form (Figure 10o and 10p). At hatching, the appearance of a carpal bone was observed in control specimens but not in experimental specimens (Figure 10q and 10r).

Using total humeral length as covariate, length of the mineralized humerus in experimental embryos was significantly greater (ANCOVA, $F_{3,80}$ =1596.738, P<0.0001) than in control embryos (Figure 11a). Similarly, length of the mineralized femur in experimental embryos was also significantly (ANCOVA, $F_{3,80}$=1149.924, P<0.0001) greater than in control embryos when plotted against total femoral length (Figure 11b). Plotting separate time points showed a significant difference (ANCOVA, $F_{3,8}$=11.374, P<0.05) in total humerus length at 33 days post-shelling between experimental (n=6) and control (n=6) embryos and continued until hatching (Table 3A). However, treatment group had no significant effect for all sample points. A significant difference (ANCOVA, P< 0.05) in total femoral length was seen in only 28, 35, 47 and 53 days post-

shelling between experimental (n=6) and control (n=6) embryos (Table 3B).

Treatment group did not show a significant effect after 21 days post-shelling.

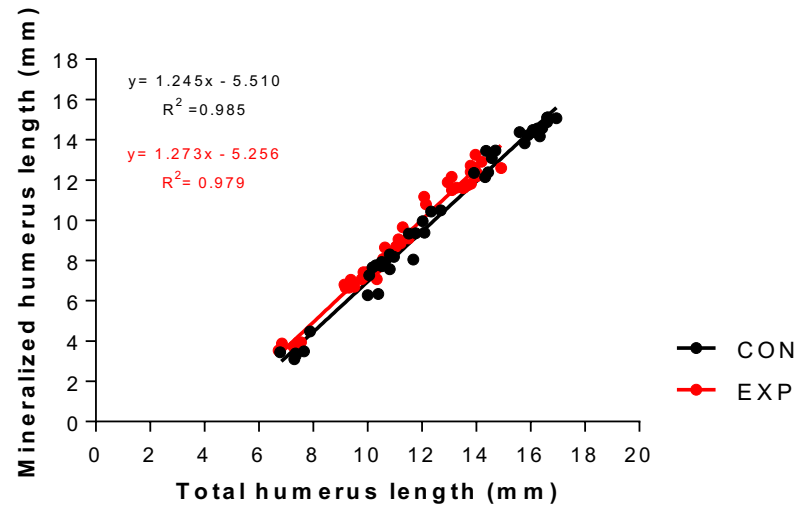

A

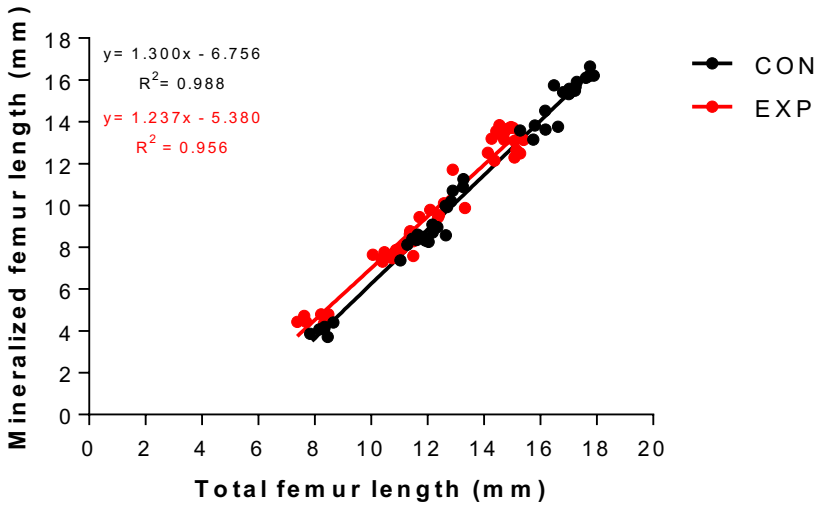

B

Figure 11. Graph of mineralized bone plotted against total length of humerus (A) and femur (B) with added linear regression. Black symbols represent data from control animals and red symbols represent data from experimental animals. A and B) For similar length of total bone,

experimental animals show a significantly (ANCOVA, $p<0.0001$) higher proportion of mineralized bone than control animals.

Table 3. ANCOVA p-values for length of mineralized humerus (A) and femur (B) against total bone length. Each sample point represents a different clutch and an n=6 for control and n=6 for experimental embryos. A) Group effect had no significant difference on length of mineralized humerus. B) Group effect had a significant difference on 21 days-post shelling but afterwards no difference was found.

	p-Value		
Days post-shelling	Total humerus length	Group	Interaction
21	0.09966	0.10487	0.35908
28	0.1009	0.27551	0.73394
33	**0.0132**	0.25818	0.11132
35	**0.01304**	0.85909	0.53564
44	**0.03792**	0.53103	0.19319
47	**0.00072**	0.2993	0.42334
53	**0.00589**	0.21719	0.25743

A

	p-Value		
Days post-shelling	Total femur length	Group	Interaction
21	0.19624	**0.00265**	0.55657
28	**0.00743**	0.59868	0.02384
33	0.16733	0.82744	0.68219
35	**0.00133**	0.20280	0.00705
44	0.25341	0.63780	0.85107
47	**0.00011**	0.36572	0.41855
53	**0.03714**	0.20602	0.94324

B

Post-hatching Growth

At hatching, total length of experimental animals was on average 7% shorter than of control hatchlings (Figure 12a). This difference in length decreased slightly (6%) by day 56. Average growth rate of total length for

experimental and control hatchlings was 0.406 mm/day and 0.388 mm/day, respectively. The initial snout-vent length of experimental hatchlings was on average 6% shorter than control hatchlings and then decreased to 5% by day 56 (Figure 12b). Average growth rate of snout-vent length for experimental and control hatchlings was 0.222 mm/day and 0.223 mm/day, respectively. The initial head length of experimental hatchlings was on average 6% shorter than control hatchlings and then decreased to a 4% difference by day 56 (Figure 12c). Average growth rate of head length for experimental and control hatchlings was 0.077 mm/day and 0.067 mm/day, respectively. Finally, the initial head width of experimental hatchlings was on average 9% shorter than control hatchlings which then decreased to a 6% difference by day 56 (Figure 12d). Average growth rate of head width in experimental and control hatchlings was 0.047 mm/day and 0.038 mm/day, respectively. Overall, the growth trajectories were parallel and body dimensions between treatment groups maintained a significant difference (ANOVA, $p<0.01$) in length with an average growth rate of 1% per week for all measured variables in both experimental and control hatchlings (Figure 12).

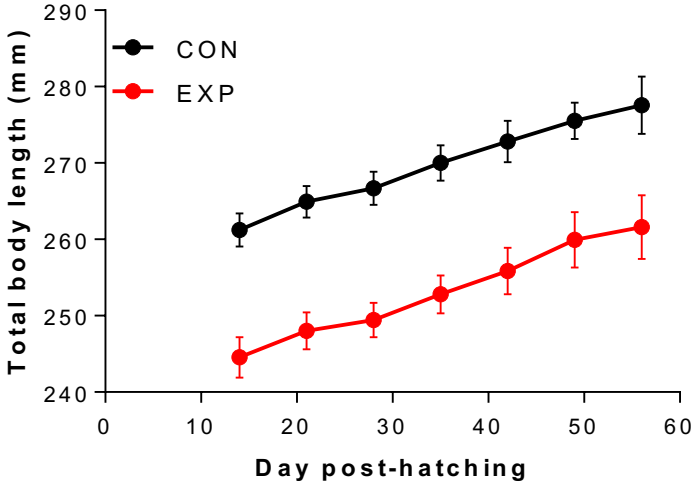

A

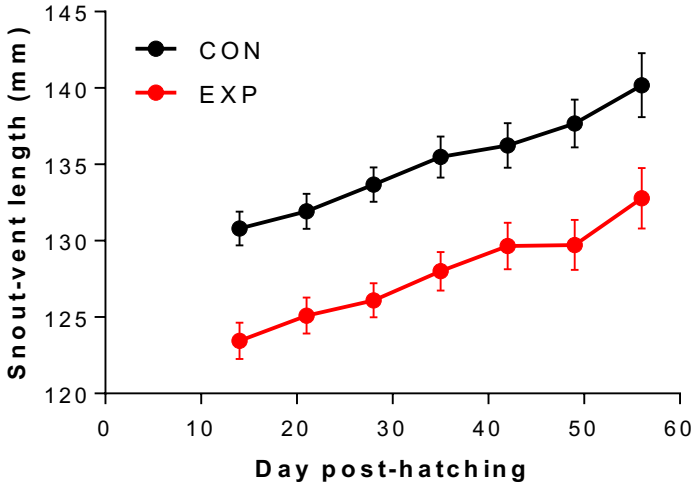

B

Figure 12. (A-D) Growth of experimental (n=29) and clutch-matched control (n=24) alligator hatchlings from the 2013 season.

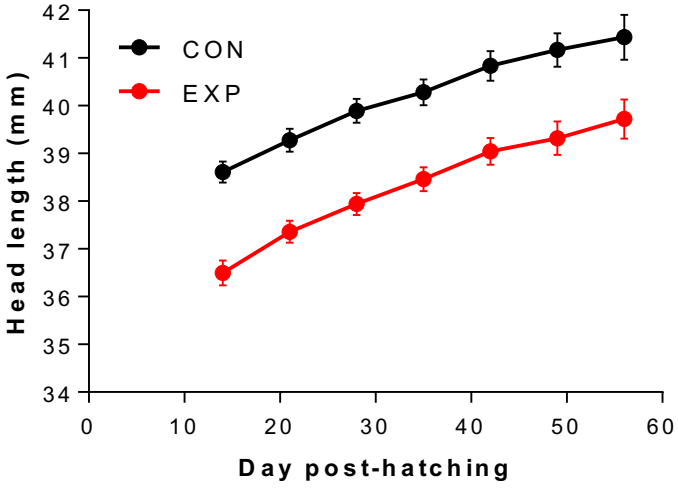

C

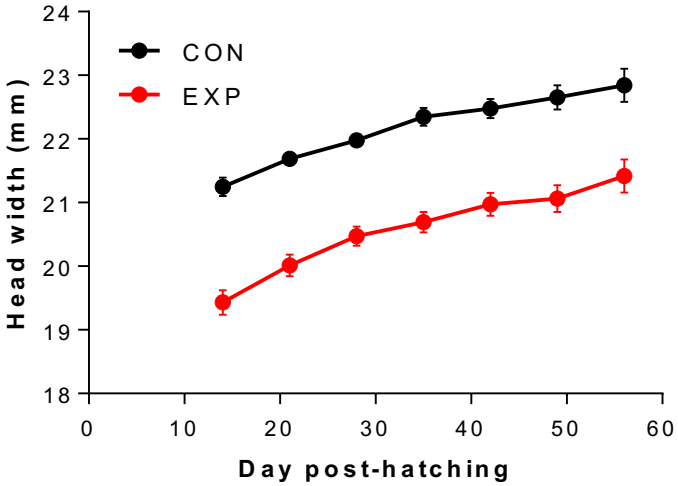

D

Figure 12 (continued). Data points are mean values, and errors bars are s.e.m. A significant difference (ANOVA, $p<0.05$) between groups is seen throughout the post-hatching measuring period. Experimental alligators did not exhibit compensatory post-hatching growth, despite an *ad libitum* diet.

Biomechanic Performance

Maximal voluntary bite force in experimental hatchlings was 81% lower than in control hatchlings (ANOVA, $F_{1,30}$=21.333, P<0.001; Figure 13a). Maximum bite torque (calculated as maximum bite force x lever arm) revealed that most experimental alligators produced significantly lower torque than similar-sized control alligators (ANCOVA, $F_{3,28}$=12.823, P<0.001; Figure 13b). Videos of voluntary biting also revealed that most experimental hatchlings had relatively compliant lower jaws (Figure 14). Upon biting, the lower jaw of experimental hatchlings deformed near the suture of the dentary and post-dentary bones. Similar deformation was not seen in control hatchlings.

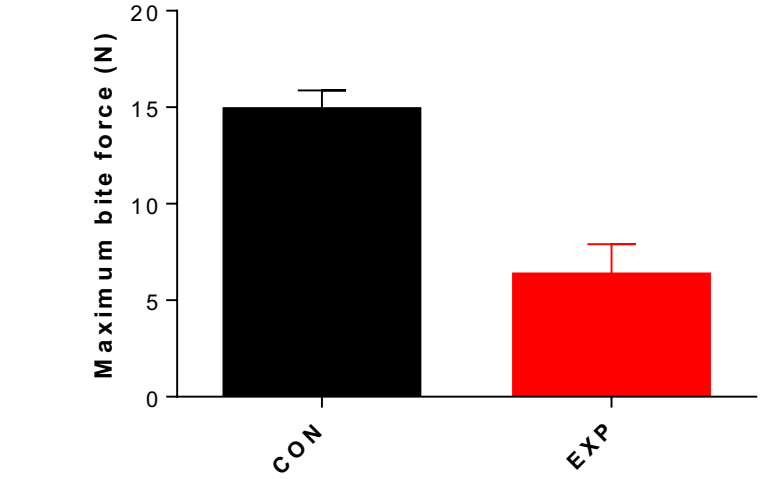

A

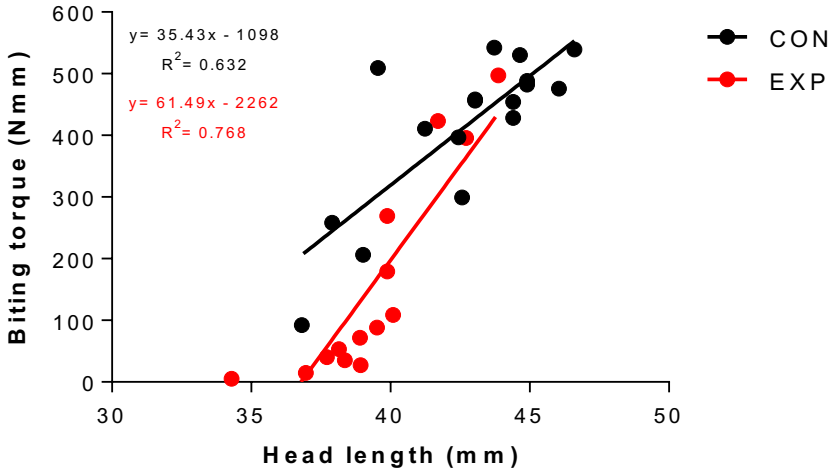

B

Figure 13. (A) Maximum voluntary bite force in three months-old alligator hatchlings from control and experimental eggs. Bars are mean, whiskers are s.e.m. Experimental animals generated an 81% lower bite force than controls (ANOVA, $p<0.001$). (B) Maximum bite torque (=bite force x lever arm) in the same two groups of alligators. Most experimental animals produced significantly lower torque than similar-sized controls (ANCOVA, head length $p<0.001$).

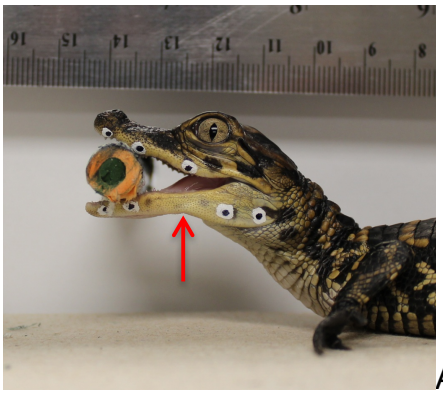
A

B

Figure 14. Lateral view of (A) an experimental hatchling (body mass=35g) and (B) control hatchling (body mass=59g) biting on a wooden dowel. Both hatchlings are age- and clutch-matched. The red arrow points to a pronounced flexion in the lower jaw of the experimental hatchling, but is not noticeable in the control animal.

Histology

Experimental hatchlings had a significantly (19%) smaller cross-sectional area (CSA) of the femoral diaphysis than control animals (ANCOVA, $F_{3,44}$=91.776, P=0.001; Figure 15a and Figure 16). Similarly, the second moment of area about the x-axis (*Ix*) (ANCOVA, $F_{3,44}$=98.846, P<0.02) and the polar moment of inertia (*J*) (ANCOVA, $F_{3,44}$=36.095, P<0.02) were also lower in experimental hatchlings (Figure 15b and 15c). Mean lacunar density of experimental hatchlings was significantly lower by 21% than control hatchlings (Wilcoxon ranked sums test, p<0.05; Figure 17).

Lower jaw CSA of experimental hatchlings was significantly lower (20%) than in control hatchlings (ANCOVA, $F_{3,45}$ =91.638, P<0.01; Figure 18a and Figure 19). However, lower jaw *Ix* and *J* reveal that there was no significant difference between treatment groups (ANCOVA, p>0.05; Figure 18b and 18c),

although *Ix* approaches significance (p=0.075). In contrast to control animals, most experimental hatchlings had large vascular spaces within the alveolar bone of the dentary (Figure 19).

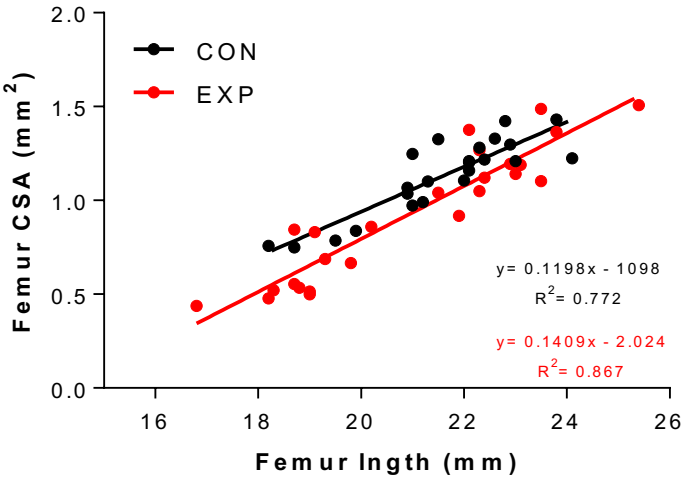

A

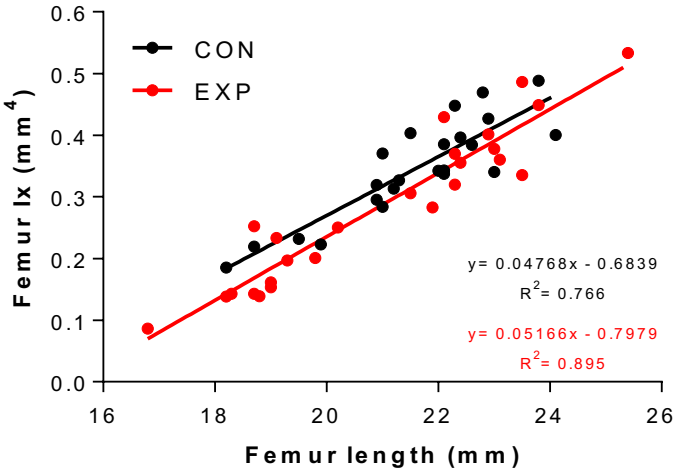

B

Figure 15. Graph of hatchling femoral cross-sectional area (CSA), second moment of area (*Ix*), and polar moment of inertia (*J*) plotted against femur length with added linear regression (A-C).

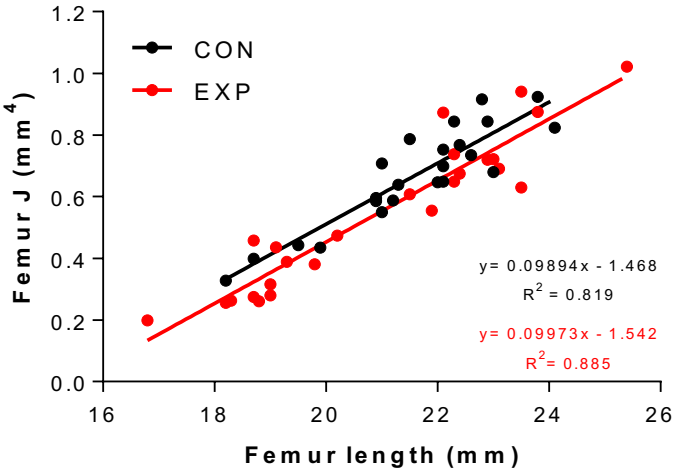

C

Figure 15 (continued). Black symbols represent data from control hatchlings and red symbols represents data from experimental hatchlings. A) Experimental hatchlings had significantly smaller CSA than controls (ANCOVA, p=0.001). B) *Ix* of experimental hatchlings was significantly lower than control hatchlings (ANCOVA, p<0.02). C) *J* of experimental hatchlings was significantly lower than control animals (ANCOVA, P<0.02).

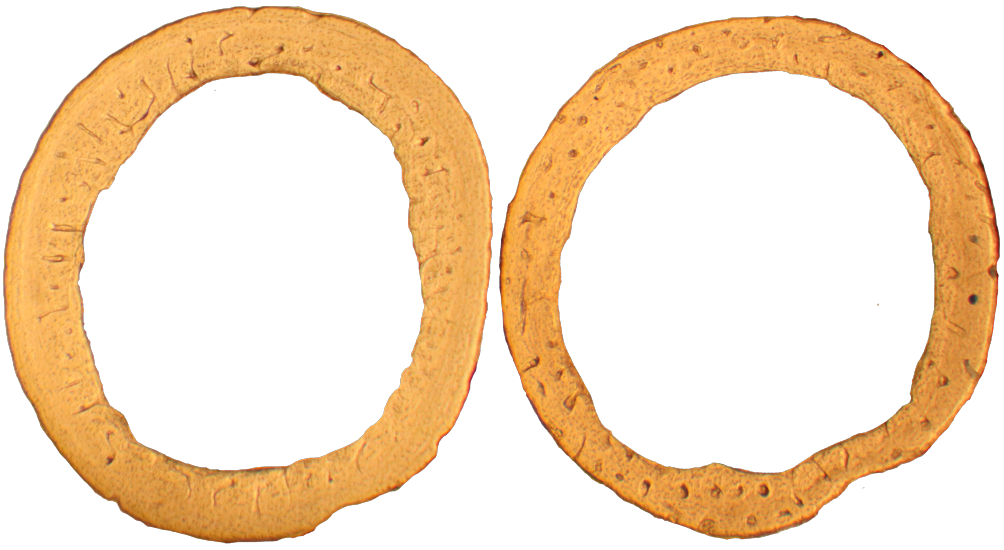

Figure 16. Cross-sectional view from the femoral mid-shaft of a control hatchling (left) and experimental hatchling (right). Cross-sections are from clutch-matched hatchlings with similar femoral

length. Note the difference in cortical thickness with experimental (right) being thinner than control (left).

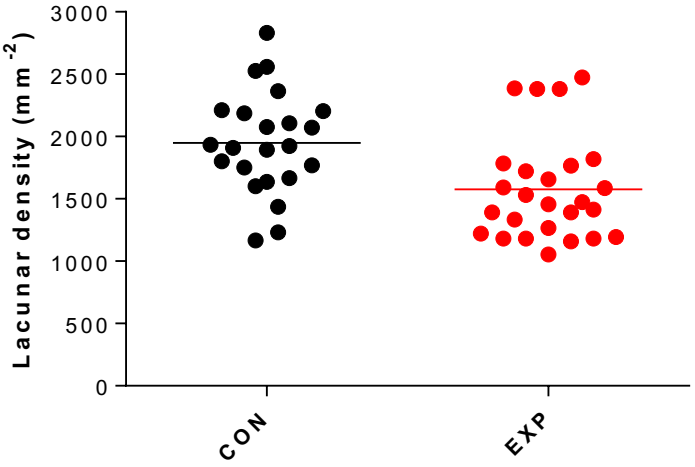

Figure 17. Plot of femoral lacunar density from control (n=23) and experimental (n=26) hatchlings. Black symbols represent control animals and red symbols represent experimental animals. Horizontal colored lines represent the mean value. Mean lacunar density from experimental animals was significantly lower than mean lacunar density of control animals (Wilcoxon ranked sums test, $p<0.05$).

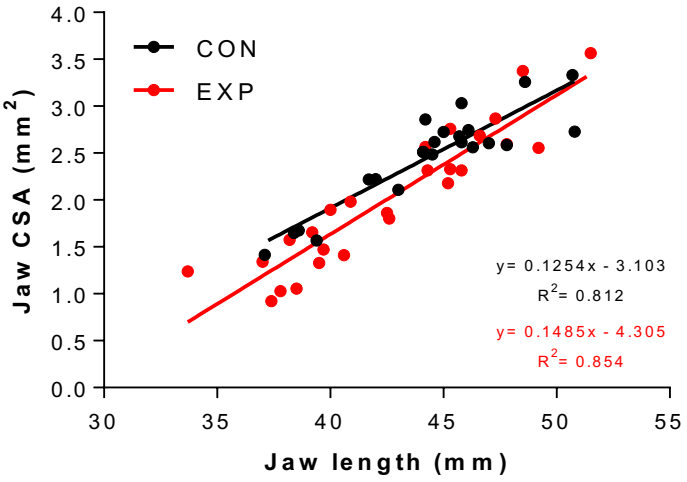

A

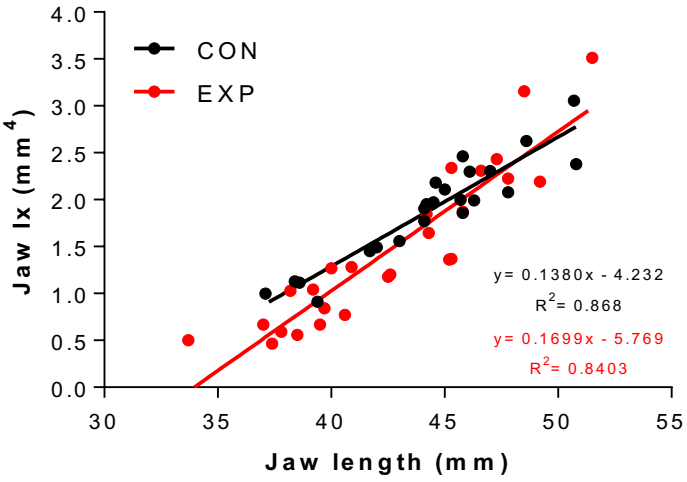

B

Figure 18. Graph of hatchling lower jaw cross-sectional area (CSA), second moment of area (*Ix*) and polar moment of inertia (*J*) plotted against jaw length with added linear regression (A-C). Black symbols represent data from control hatchlings and red symbols represent data from experimental hatchlings.

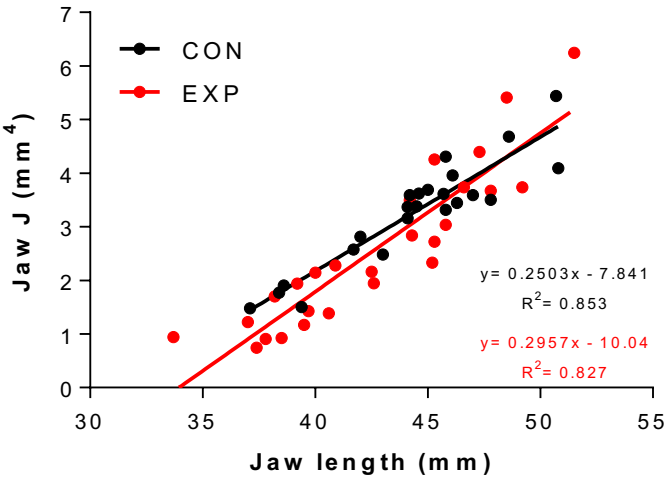

C

Figure 18 (continued). A) Experimental hatchling jaw CSA was significantly smaller than controls (ANCOVA, p=0.011). B and C) No significant difference in *Ix* and *J* between control and experimental animals (ANCOVA, p=0.075 and p>0.05, respectively).

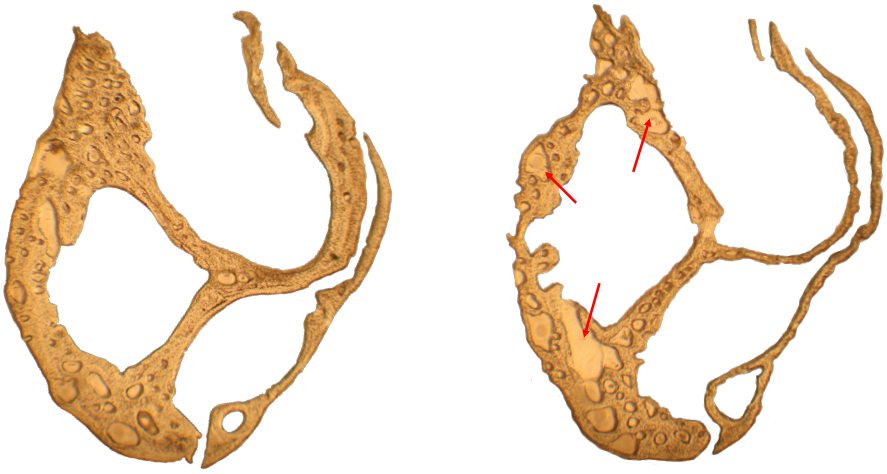

Figure 19. Cross-sectional view of a control (right) and experimental (left) hatchling lower jaw taken from the middle of the dentary and splenial bone. Cross-sections are from clutch-matched siblings with equal jaw lengths. Note that the dentary bone from the experimental hatchling contains large vascular spaces as indicated by the red arrows. Vascular spaces in jaws from control hatchlings were much less prominent

CHAPTER FOUR

DISCUSSION

Despite experimental removal of the calcareous eggshell, embryos of the American alligator were able to develop and grow to hatching. Absence of the calcium reservoir resulted in significantly reduced embryonic growth, which produced diminutive hatchlings compared to clutch-matched control animals. This suggests that at the time of peeling (Ferguson stage 15) the calcareous layer there is sufficient calcium reserves in the yolk sac for skeletogenesis. My experimental results support the hypothesis by Packard & Seymour (1997) that loss of calcium source (the eggshell) constrains embryonic growth rate and leads to diminutive hatchlings. The reduction in growth explains the consistently heavier yolk sacs in experimental hatchlings during incubation after eggshell removal (Figure 4b and 4d). Owerkowicz et al. (2009) reports a similar observation with their hypoxic incubated hatchling alligators having large internalized yolk sacs. They posit that the low oxygen concentration reduces embryonic metabolic rate and therefore the embryos cannot catabolize yolk material to the same extent as normoxic incubated embryos. In my study, metabolic rate was not measured and as to why experimental embryos did not just deplete the yolk sac of calcium for normal skeletal growth remains to be further investigated. Although experimental embryos had more yolk ash mineral mass towards the end of incubation (Figure 8), when taken as proportion of total

dry yolk mass, experimental embryos have significantly lower ash mineral content than controls (Figure 9), i.e., lower mineral concentration. This is consistent with Packard's (1994) observation that alligator embryos mobilize eggshell calcium into the yolk sac towards the end of incubation.

Measurements taken from eggshells show a general decrease in thickness. Thickness at the poles is significantly lower than at the equator throughout incubation (Figure 7). The linear regression equation for the poles shows that the polar regions decrease faster than the equatorial regions. This is counterintuitive since the chorioallantoic membrane (CAM) spreads from the equatorial region to the polar region, and therefore should mobilize more calcium from the equatorial region of the egg. Whether there is a disproportion of calcium transport pumps around the CAM remains to be investigated. Therefore, these result reject the hypothesis that eggshell thickness decreases uniformly throughout the egg. Furthermore, this observation is different from that of chicken eggs whereby the poles are thicker than the equator (Tyler and Geake, 1965). Generally, bird eggs have one pole that is narrower than the other which helps prevent it from rolling out of the nest (Smart, 1991). Additionally, most birds incubate their eggs by sitting on them. These eggs can resist more mechanical loading across the long axis (pole-to-pole) than the equator (Hahn et al., 2017). In contrast, alligator eggs are elliptical and are deposited on top of each other in a mound of vegetation (Ferguson, 1985). Having a thicker eggshell around the equatorial region may help prevent the eggs from mechanical damage when

being deposited. Megapode birds are the only known birds to incubate their eggs in a similar manner to crocodilians. Most eggs of megapode birds have an elliptical shape and all eggs are incubated in mounds of vegetation or sand (Jones et al., 1995). Compared to similar sized eggs from other bird species, megapode eggshell is 31% thinner (Booth and Thompson, 1991). Unlike crocodilians, megapode birds do not lay their eggs simultaneously but rather individually over the span of their breeding period (Seymour and Akerman, 1980). Therefore, megapode eggs may not experience much mechanical damage regardless of having a thin eggshell when deposited in the nest.

The series of cleared and stained embryos from the 2012 summer season reveal that removal of the calcareous eggshell did not affect the onset of bone mineralization in experimental embryos. These results reject the hypothesis that eggshell removal delays onset of bone mineralization. No bone is observed to have started mineralizing by stage 19 (Figures 10a and 10b). In contrast to my results, Rieppel (1993) reported that some bones of the alligator dermatocranium (e.g. pterygoid) begin to mineralize as early as stage 18. Dermal bones such as the pre-maxilla, maxilla, and dentary begin to mineralize during stage 19. Additionally, the mid-diaphysis of the stylopodium and zeugopodium also start to mineralize during stage 19 (Rieppel, 1993). In contrast to Rieppel's (1993) study, Vickaryous and Hall (2008) show that most bones of the alligator dermatocranium mineralize a stage earlier than what was previously known. For example, the pterygoid is seen to start mineralizing at stage 17. The surangular

and lacrimal are the only bones shown to mineralize at the same stage as reported in Rieppel's (1993) study.

In this study, mineralization of these same bones are observed by stage 21 in both experimental and control embryos (Figure 10c and 10d). It is possible that mineralization of these bones would have been observed during early stage 20 but no embryos were sampled at that stage. The remaining post-cranial skeleton is mineralized in subsequent embryonic stages. The only difference in time of bone mineralization is observed at hatching, when carpal bones show mineralization in control animals but not in experimental animals. Presumably experimental animals would have mineralized this bone a little later after hatching. One possible explanation as to why bone mineralization is seen later than what is previously reported may be due to staining with Alcian blue. Vickaryous and Hall (2008) stated that their specimens stained better for Alizarin red when Alcian blue was omitted. The glacial acetic acid found in the Alcian blue solution may serve as source of decalcification. In both this study and Rieppel's (1998) study, all specimens underwent double staining with Alizarin red and Alcian blue. In this study, all specimens were first stained with Alcian blue and then later stained with Alizarin red.

During the latter half of incubation, experimental embryos have significantly shorter humeri and femora than control embryos (See Appendix A). Despite lacking the calcareous eggshell, experimental embryos are able to mineralize similar proportion of their bones compared to control embryos. At

hatching (53 days post-shelling), experimental alligators have on average 88% of their humerus and 90% of their femur mineralized, compared to control alligators which have on average 90% of their humerus and 92% of their femur mineralized. However, the difference in percentage between experimental and control hatchlings is not significant for percent-mineralized humerus (ANOVA, $F_{1,10} = 4.7468$, $P>0.05$) and percent-mineralized femur (ANOVA, $F_{1,10} =0.1114$, $P>0.05$). This would suggest that timing of mineralization is under genetic control. Furthermore, whether this slight difference results in biomechanic and behavioural differences remains to be studied.

Packard and Seymour (1997) suggested that embryos which are denied access to eggshell calcium will hatch smaller in size than those that can utilize eggshell calcium. This prediction is supported by the results of this study. Furthermore, experimental hatchlings in this study did not show compensatory growth by the end of a two-month post-hatching period (Figure 12), which allows me to reject the hypothesis that experimental hatchlings will match control hatchlings in size. Over the span of two months, both treatment groups grew an average of 1% per week for all measured variables. This same rate of growth may explain why experimental hatchlings remained consistently smaller throughout the experiment. A 56-day growth period of normoxic hatchling alligators from Owerkowicz et al. (2009) reported a two to three times faster growth rate for total length, snout-vent length, head length, and head width than hatchlings from this study (See Appendix B). This considerable difference in

growth rate may be due in part to the feeding schedule and type of food hatchlings received in both experiments. Hatchlings in this study were fed crushed pellets (Lone Star® alligator food) twice a week. In contrast, hatchlings from Owerkowicz et al. (2009) were fed lean ground beef sprinkled with powdered mineral/vitamin every other day. Having access to food more frequently may have allowed the normoxic hatchlings to grow faster.

Bite forces in *Alligator mississippiensis* had been shown to scale with positive allometry with respect to increasing body size (Erickson et al., 2003). In this study, maximal bite force for experimental hatchlings is 81% lower than max bite force from controls. Therefore, these results support the hypothesis that experimental hatchlings will produce a weaker bite force than controls. Using the linear regression equation y=2.75x+(-0.65) from the Erickson et al. (2003) study provides the predicted bite force (N) for a given head length (mm). No significant difference (ANOVA, p=0.1445, F-ratio= 2.2371) is shown when comparing actual bite force versus predicted bite force in control hatchlings. In contrast, experimental hatchlings produce a significantly lower (ANOVA, p=0.0016, F-ratio=12.4598) bite force than what is predicted for a given head length. Interestingly, most experimental hatchlings have flexible lower jaws, which may suggest that their lower jaw is not yet mineralized to the same extent as that of control animals. Having a flexible lower jaw would have reduced maximal biting torque of experimental hatchlings. Ventral flexion of the lower jaw was not observed in control hatchings, and I have not been able to quantify stiffness of

the mandible. Erickson et al. (2003) reported flexion on the balancing side of the lower jaw in wild hatchling alligators during voluntary biting of a force transducer. These hatchling alligators, however, were biting the force transducer unilaterally. Hatchlings in this study bit the force transducer bilaterally and no flexion is observed besides that in the post-dentary region of the lower jaw of experimental hatchlings. In the wild, the main diet of hatchlings consists of insects and small fish (Dodson, 1975). An experimental hatchling from this study may find it difficult to successfully capture prey due to its reduced bite-force capability and flexible lower jaw.

Histological cross-sections taken from the middle of their lower jaw reveal experimental hatchlings have a reduced cross-sectional area (CSA) with large vascular spaces in the dentary bone. This may be another reason why experimental hatchlings could not produce stronger bite forces. No difference in *Ix* and *J* is observed between experimental and control hatchlings. Both *Ix* and *J* are a function of the cross-sectional area and its distribution around the neutral axis (Vogel, 2003). However, the theoretical location (calculated by Image J) of the neutral axis may be different from its actual location in the jaw, which varies with magnitude and orientation of forces acting on it during dynamic biting. It is possible that the distribution of material in the lower jaw of experimental hatchlings may have slightly shifted during the embedding process or grinding of the slide, thereby increasing bone distribution from the neutral axis in cross-section, and thus artificially augmenting *Ix* and *J*. This may be a reason why no

significant difference is observed in *Ix* and *J* between experimental and control hatchlings.

Cross-sections taken from the mid-diaphysis of hatchling femora also reveal that experimental CSA is significantly reduced compared to controls (Figure 15a). In contrast to the *Ix* and *J* of the lower jaw, experimental hatchlings had a significantly reduced femoral *Ix* and *J* compared to control hatchlings (Figure 15b and 15c). This suggest that the femora of control hatchlings have a higher resistance to bending and torsion. These results partially (with exception to *Ix* and *J* of the lower jaw) support the hypothesis that experimental hatchlings will have a reduced CSA, *Ix* and *J* compared to control hatchlings. How this affects actual bone mechanical performance (e.g. mechanical failure) remains to be tested.

When looking at mean lacunar density, experimental hatchlings have a 21% lower concentration of lacunae than controls (Figure 17). In compact bone, osteoblast can lay down concentric layers of bone in the form of lamellae. As the osteoblast continue to lay successive layers of lamellae they become trapped in spaces called lacunae (Wheater et al., 1987). A reduced number of lacunae may indicate a reduction of mineral density. Whether femoral mineral density in experimental hatchlings is lower than in similarly-size control animals remains to be determined.

The results of this project support the overall hypothesis that removal of the calcareous eggshell would produce small hatchlings with reduced

biomechanic performance. The results suggest that eggshell calcium is important for proper embryonic growth in the American alligator, but sufficient calcium reserves are found in the yolk. The evolution of the calcareous eggshell not only serves as a protective barrier against desiccation and infection, but also as an essential source of calcium for producing a large hatchling with a well-mineralised skeleton.

APPENDIX A

AVERAGE LENGTH OF TOTAL BONE AND MINERALIZED BONE FOR HUMERI (A) AND FEMORA (B) DURING EACH TIME POINT

Table 4. Average length of total bone and mineralized bone for humeri (A) and femora (B) during each time point. A different clutch of eggs (experimental=6 and control=6) was sampled at each time point.

A

Days post-shelling	Average total humerus length (mm)		Average mineralized length (mm)	
	Control	Experimental	Control	Experimental
21	7.39	7.22	3.53	3.79
28	10.35	9.58	7.16	7.03
33	10.80	9.97	7.99	7.26
35	12.07	11.14	9.82	9.00
44	14.39	13.25	12.81	11.58
47	16.44	13.36	14.62	12.29
53	16.11	14.04	14.50	12.29

B

Days post-shelling	Average total femur length (mm)		Average mineralized length (mm)	
	Control	Experimental	Control	Experimental
21	8.30	7.96	4.06	4.59
28	11.48	10.56	8.23	7.64
33	12.22	11.21	8.65	8.08
35	12.94	12.42	10.49	9.69
44	15.97	15.03	13.75	12.53
47	17.22	14.26	15.71	13.23
53	17.30	14.83	15.90	13.28

APPENDIX B

COMPARISON OF GROWTH RATES FROM EXPERIMENTAL AND CONTROL HATCHLINGS TO A 56-DAY GROWTH PERIOD OF HATCHLING ALLIGATORS RAISED UNDER NORMAL OXYGEN CONDITION

Table 5. Comparison of growth rates from experimental and control hatchlings to a 56-day growth period of hatchling alligators raised under normal oxygen condition. (*) Data on growth measurements for the same post-hatching period was acquired with permission from Owerkowicz et al. (2009). Experimental and control hatchlings have similar growth rates for all measured variables. However, growth rates of hatchlings from this study are slower than those of the control hatchlings from the Owerkowicz et al. (2009) study.

	TL (mm/day)	SVL (mm/day)	HL (mm/day)	HW (mm/day)
Control	0.388	0.223	0.067	0.038
Experimental	0.406	0.22	0.077	0.047
Normoxic *	1.2	0.52	0.138	0.071

REFERENCES

Board, R.G., and N.H.C. Sparks. 1991. Shell structure and formation in avian eggs. Pages: 71-86 in: *Egg Incubation: Its Effects on Embryonic Development in Birds and Reptiles* (D.C. Deeming and M. W. J. Ferguson, eds.). Cambridge, UK: Cambridge University Press.

Booth, D.T. and M.B. Thompson. 1991. A comparison of reptilian eggs with those of megapode birds. Pages: 325-345 in: *Egg Incubation: Its Effects on Embryonic Development in Birds and Reptiles* (D.C. Deeming and M. W. J. Ferguson, eds.). Cambridge, UK: Cambridge University Press.

Cree, A., L.J. Guillette, JR. and K. Reader. 1996. Eggshell formation during prolonged gravidity of the tuatara *Sphenodon punctatus*. *Journal of Morphology* **230**:129-144.

D'Alba, L., D.N. Jones, H.T. Badawy, C.M. Eliason and M.D. Shawkey. 2014. Antimicrobial properties of a nanostructured eggshell from a compost-nesting bird. *The Journal of Experimental Biology* **217:**1116-1121.

Deeming, D.C. and M.W.J. Ferguson. 1989. Effects of incubation temperature on growth and development of embryos of *Alligator mississippiensis*. *Journal of Comparative Physiology B* **159**:183-193.

Dodson, P. 1975. Functional and ecological significance of relative growth in *Alligator*. *Journal of Zoology (Lond.)* **175**:315-355.

Dunn, B.E. 1991. Methods for shell-less and semi-shell-less culture of avian and reptilian embryos. Pages:409-418 in: *Egg Incubation: Its Effects on Embryonic Development in Birds and Reptiles* (D.C. Deeming and M. W. J. Ferguson, eds.). Cambridge, UK: Cambridge University Press.

Ecay, T.W., J.R. Stewart and D.G. Blackburn. 2004. Expression of calbindin-D_{28K} by yolk sac and chorioallantoic membranes of the corn snake, *Elaphe guttata*. *Journal of Experimental Zoology* **302B**:517-525.

Erickson, G.M., A.K. Lappin and K.A. Vliet. 2003. The ontogeny of bite-force performance in American alligator (*Alligator mississippiensis*). *Journal of Zoology, London* **260**: 317-327.

Ferguson, M.W.J. 1985. The reproductive biology and embryology of crocodilians. Pages 329-491 In: *Biology of the Reptilia*: *Development* A (C. Gans, F. Billet, and P. F. A. Maderson, Eds). New York: John Wiley and Sons.

Fischer, R.U., F.J. Mazzotti, J.D. Congdon and R.E. Gatten, Jr. 1991. Post-hatching yolk reserves: parental investment in American alligators from Louisiana. *Journal of Herpetology* **25**:253-256.

Hahn, E.N., V.R. Sherman, A. Pissarenko, S.D. Rohrbach, D.J. Fernandes and M.A. Meyers. 2017. Nature's technical ceramic: the avian eggshell. *Journal of the Royal Society Interface*. **14**: 20160804.

Hincke, M.T., Y. Nys, J. Gautron, K. Mann, A.B. Rodriguez-Navarro and M.D. McKee. 2012. The eggshell: structure, composition and mineralization. *Frontiers in Bioscience* **17:**1266-1280.

Hirsch, K.F. 1983. Contemporary and fossil chelonian eggshells. *Copeia* **1983(2)**:382-397.

Hoenderop, J.G.J., B. Nilus and R.J.M. Bindels. 2005. Calcium absorption across epithelia. *Physiological Reviews **85:**373-422.*

Hughes, R.L. 1984. Structural adaptations of the eggs and the fetal membranes of monotremes and marsupials for respiration and metabolic exchange. Pages 389-421 in: *Respiration and Metabolism of Embryonic Vertebrates* (R. S. Seymour, ed.). Dordrecht: Dr W. Junk Publishers.

Jones, D.N., R.W. Dekker and C.S. Roselaar. 1995. General biology and behavior. Pages: 33-43 in: *The Megapodes: Megapodiidae*. Oxford, New York, and Tokyo: Oxford University Press.

Lappin, A.K. and M.E. Jones. 2014. Reliable quantification of bite-force performance requires use of appropriate biting substrate and standardization of bite out-lever. *Journal of Experimental Biology* **217**:4303-4312.

Leary, S., W. Underwood, R. Anthony, S. Cartner, D. Corey, T. Grandin, C. Greenacre, S. Gwaltney-Brant, M.A. McCrakin, R. Meyer, D. Miller, J. Shearer and R. Yanong. 2013. AVMA guidelines for the euthanasia of animals. 2013 edition pg.1-102.

Marzola, M., J. Russo and O. Mateus. 2014. Identification and comparison of modern and fossil crocodilian eggs and eggshell structures. *Historical Biology* **27**:115-133.

Needham, J. 1931. *Chemical Embryology*. Cambridge: Cambridge University Press.

Owerkowicz, T., R.M. Elsey and J.W. Hicks. 2009. Atmospheric oxygen level affects growth trajectory, cardiopulmonary allometry and metabolic rate in the American alligator (*Alligator mississippiensis*). *Journal of Experimental Biology* **212**:1237-1247.

Packard, G.C. 1999. Water relations of chelonian eggs and embryos: is wetter better? *American Zoology* **39**:289-303.

Packard, G.C. and M.J. Packard. 1980. Evolution of the cleidoic egg among reptilian antecedents of birds. *American Zoology* **20**:351-362.

Packard, M.J. 1994. Patterns of mobilization and deposition of calcium embryos of oviparous, amniotic vertebrates. *Israel Journal of Zoology* **40**:481-492.

Packard, M.J. and N.B. Clark. 1996. Aspects of calcium regulation in embryonic lepidosaurians and chelonians and a review of calcium regulation in embryonic archosaurians. *Physiological Zoology* **69**:435-466.

Packard, M.J. and G.C. Packard. 1991. Sources of calcium, magnesium and phosphorus for embryonic softshell turtles (*Trionyx spiniferus*). *The Journal of Experimental Zoology* **258**:151-157
.

Packard, M.J. and G.C. Packard. 1989. Mobilization of calcium, phosphorus, and magnesium by embryonic alligators (*Alligator mississipiensis*). *American Journal of Physiology* **257**:R1541-R1547.

Packard, M.J. and G.C. Packard. 1988. Sources of calcium and phosphorus during embryogenesis in bullsnakes (*Pituophis melanoleucus*). *The Journal of Experimental Zoology* **246**:132-138.

Packard, M.J. and G.C. Packard. 1984. Comparative aspects of calcium metabolism in embryonic reptiles and birds. Pages 155-179 in: *Respiration and Metabolism of Embryonic Vertebrates* (R. S. Seymour, ed.). Dordrecht: Dr W. Junk Publishers.

Packard, M.J., G.C. Packard and T.J. Boardman. 1982. Structure of eggshells and water relations of reptilian eggs. *Herpetologica*. **38**:136-155.

Packard, M.J., G.C. Packard and W.H.N. Gutzke. 1984. Calcium metabolism in embryos of the oviparous snake *Coluber constrictor*. *Journal of Experimental Biology* **110**:99-112.

Packard, M.J. and R.S. Seymour. 1997. Evolution of the amniote egg. Pages 265-290 in: *Amniote Origins: Completing the Transition to Land* (S. S.

Sumida and K. L. M. Martin, eds.). Sand Diego and New York: Academic Press.

Packard, M.J. and V.G. DeMarco. 1991. Eggshell structure and formation in eggs of oviparous reptiles. Pages 53-69 in: *Egg Incubation: Its Effects on Embryonic Development in Birds and Reptiles* (D.C. Deeming and M. W. J. Ferguson, eds.). Cambridge, UK: Cambridge University Press.

Rieppel, O. 1993. Studies on skeletal formation in reptiles. v. Patterns of ossification in the skeleton of *Alligator mississippiensis* DAUDIN (Reptilia, Crocodylia). *Zoological Journal of the Linnean Society* **109**:301-325.

Seymour, R.S. and R.A. Ackerman. 1980. Adaptations to underground nesting in birds and reptiles. *Amer. Zool.* **20**:437-447.

Seymour, R.S. and D.F. Bradford. 1995. Respiration of amphibian eggs. *Physiological Zoology* **68**:1-25.

Smart, I.H. 1991. Egg shape in birds. Pages 101-116 in: *Egg Incubation: Its Effects on Embryonic Development in Birds and Reptiles* (D.C. Deeming and M. W. J. Ferguson, eds.). Cambridge, UK: Cambridge University Press.

Song, J. and L.R. Parenti. 1995. Clearing and staining whole fish specimens for simultaneous demonstration of bone, cartilage, and nerves. *Copeia* **1995**:114-118.

Stewart, J.R., T.W. Ecay, B. Heulin, S.P. Fregoso and B.J. Linville. 2011. Developmental expression of calcium transport proteins in extraembryonic membranes of oviparous and viviparous *Zootoca vivipara* (Lacertilia, Lacertidae). *Journal of Experimental Biology* **214**:2999-3004.

Stewart, J.R. 1997. Morphology and evolution of the egg of oviparous amniotes. Pages 291-326 in: *Amniote Origins: Completing the Transition to Land* (S. S. Sumida and K. L. M. Martin, eds.). San Diego and New York: Academic Press.

Trauth, S.E. and W.R. Fagerberg. 1984. Ultrastructure and stereology of the eggshell in *Cnemidophorus sexlineatus* (Lacertilia: Teiidae). *Copeia* **1984(4)**:826-832.

Tong, H., P. Wan, W. Ma, G. Zhong, L. Cao, and J. Hu. 2008. Yolk spherocrystal: the structure, composition and liquid crystal template. *Journal of Structural Biology* **163**:1-9.

Tuan, R.S. 1991. Experimental studies on cultured, shell-less fowl embryos: calcium transport, skeletal development, and cardio-vascular functions. Pages 419-433. In: *Egg Incubation: Its Effects on Embryonic Development in Birds and Reptiles* (D.C. Deeming and M. W. J.. Ferguson, eds.). Cambridge, UK: Cambridge University Press.

Tyler, C. and F.H. Geake. 1965. Thickness and patterns as shown by individual domestic hens. *British Poultry Science* **6**:235-243.

Vickaryous, M.K. and B.K. Hall. 2008. Development of the dermal skeleton in *Alligator mississippiensis* (Achosauria, Crocodylia) with comments on homology of osteoderms. *Journal of Morphology*. **269**:398-422.

Vogel, S. 2003. Simple structures: beams, columns, shells. Pages:365-405 in: *Comparative Biomechanics: Life's Physical World*. Princeton and Oxford: Princeton University Press.

Wassersug, R. 1976. A procedure for differential staining of cartilage and bone in whole formalin-fixed vertebrates. *Stain Technology* **51**:131-134.

Wheater, P.R., H.G. Burkitt and V.G. Daniels. 1987. Skeletal Tissue. Pages 142-160 in: *Functional Histology: A Text and Colour Atlas – 2nd ed.* (P.R. Wheater and HG. Burkitt, eds.) Edinburgh: Churchill Livingstone.